NTIA Report 95-325

Building Penetration Measurements From Low-height Base Stations At 912, 1920, and 5990 MHz

Lynette H. Loew
Yeh Lo
Michael G. Laflin
Elizabeth E. Pol

U.S. DEPARTMENT OF COMMERCE
Ronald H. Brown, Secretary

Larry Irving, Assistant Secretary
for Communications and Information

September 1995

PRODUCT DISCLAIMER

Certain commercial companies, equipment, instruments, and materials are identified in this paper to specify adequately the technical aspects of the reported results. In no case does such identification imply recommendation or endorsement by the National Telecommunications and Information Administration, nor does it imply that the material or equipment identified is necessarily the best available for the purpose.

CONTENTS

CONTENTS (cont'd)

Page

FIGURES

Page

FIGURES (cont'd)

Page

FIGURES (cont'd)

Page

FIGURES (cont'd)

Page

FIGURES (cont'd)

Page

TABLES

TABLES (cont'd)

Page

GLOSSARY OF TERMS

The following terms are described in order to avoid confusion and make clear the procedures employed during the gathering and analysis of the data presented in this report. They are not necessarily identical to the complete, rigorous or mathematical definitions of the terms.

building penetration loss
The ratio in median signal strength between the measurement obtained inside the building and the reference signal level measured outside the building at street level. This interpretation of building penetration is similar to that given by the International Telecommunication Union-Radiocommunications (ITU-R), formerly CCIR [1].

high-rise building
A multistory office building in an urban environment.

line-of-sight transmission path
A straight line path between the transmitter and building under test which is not obstructed by any buildings.

median value
The median value of the path loss measurements in one area, such as one room within a building or one corner of a high-rise building.

mean value
The average value of the medians calculated for all rooms in a residence and all corners for each level of a high-rise building.

non-line-of-sight transmission path
A straight line path between the transmitter and building under test that is obstructed by at least one building.

path loss
Attenuation undergone by an electromagnetic wave in transit between a transmitter and receiver. In this report, path loss refers to the median loss experienced, calculated from the received signal level.

reference signal level
The median of the line-of-sight field intensity measured at street level outside the wall of the building under test closest to the transmitter. If the transmitter is nearest to a corner of the building under test, we use the average value of the measurement of the two walls that make up that corner.

residential building
A single family house in a suburban area.

BUILDING PENETRATION MEASUREMENTS FROM LOW-HEIGHT BASE STATIONS AT 912, 1920, AND 5990 MHz

Lynette H. Loew[1], Yeh Lo[1], Michael G. Laflin[1], and Elizabeth E. Pol[2]

Building penetration measurements were taken simultaneously at three potential Personal Communications Services (PCS) frequencies: 912, 1920, and 5990 MHz. The continuous wave (CW) measurement system employed a fixed outdoor transmitter and a mobile indoor receiver. The goal was to quantify building penetration losses at these frequencies to determine the viability of indoor coverage using street microcells and base antenna heights below the roof level of surrounding buildings. Eleven different buildings representing typical residential and high-rise office building environments were used for the measurements. Vertically polarized transmit and receive antennas were used for all measurements. Statistical analyses of the data include mean building attenuation losses, standard deviations, cumulative probability distribution functions, and correlation coefficients. The analyses were used to characterize propagation effects and provide a comparison between three frequencies, two cell environments, and two transmission paths.

Key Words: *attenuation; building attenuation; building penetration; measurements; personal communications services; PCS; penetration characteristics; penetration loss; radio propagation*

1. INTRODUCTION

The mobile communications community has great interest in improving cellular system performance and developing new telecommunication services such as Personal Communications Services (PCS) and advanced cellular mobile systems. A significant system improvement would be the ability to use one mobile communication system in an uninterrupted manner both inside and outside buildings. If an outdoor microcell could provide coverage to indoor subscribers, it would be unnecessary to place base stations inside each building requiring coverage. This would eliminate the problems of handoff from the outdoor to the indoor transmitter, and reduce the costs of the system. Indoor picocell design would no longer be required. Locating the outdoor base station on an existing structure, such as a street or traffic light, would be particularly advantageous. To determine the viability of indoor coverage from an outdoor base station at

[1]The authors are with the Institute for Telecommunication Sciences, National Telecommunications and Information Administration, U.S. Department of Commerce, Boulder CO 80303.

[2] The author is no longer employed with the Institute for Telecommunications Sciences.

traffic-light height, this paper presents the results of narrowband building penetration measurements (see Glossary of Terms) made in Boulder and Denver, Colorado, in the spring of 1993. The geometry of the test configurations suggests that the radio signals penetrated the buildings mainly via walls and windows, due to the low base antenna height (5 m).

The measurements were taken in residential and high-rise buildings (see Glossary of Terms) at 912, 1920, and 5990 MHz. Included in the measurements were all levels of the residences (including basements), and seven or eight nonconsecutive levels of the high rises, up to a maximum of the fifteenth level. The building penetration measurement system consisted of a three-frequency fixed transmitter positioned 25 to 200 m from the receiver. The transmitter was set at a height of 5 m to simulate the height of a street or traffic light. The receiver was held at a height of 1.9 m to simulate the height of a person using a phone. Path loss (see Glossary of Terms) data at 912, 1920, 5990 MHz were collected simultaneously as the receiver was moved inside the building under test. Data were recorded at 16-ms sampling intervals for a 50-s period while the receiver moved at an approximate speed of 0.75 m/s. At this speed/sampling interval we captured at least eight samples per wavelength, to ensure that we collected data during the deep fades which can be encountered every half-wavelength due to multipath. We recorded fades of up to 30 dB even at the highest frequency (see Figure 32).

The path loss data were analyzed to provide building attenuation statistics. The results of this data analysis provide a comparison between the three frequencies, two cell types, two transmission paths, and various floor heights of high-rise buildings.

2. MEASUREMENT SYSTEM

The measurement system configuration selected was advantageous because it allowed simultaneous measurement of received signal levels at multiple frequencies using a single communication channel. Using this method, we were ensured of obtaining signals at all frequencies which have been transmitted through exactly the same obstructions at exactly the same time. Thus, the analysis of building penetration loss as a function of frequency was expected to be more reliable than could be achieved using other testing configurations.

2.1 Equipment Description

The system consisted of a fixed transmitter and a mobile receiver. The transmitter was located on the street near the building under test, emulating a microcell base station. The receiver was carried manually throughout the building under test. The maximum distance from transmitter to receiver was restricted to 300 m in order to keep the received signal strength within the dynamic range of the low-power test equipment.

2.1.1 Transmitter

A vertically polarized, omnidirectional antenna was used to transmit three frequencies simultaneously. The antenna was positioned at a height of 5 m by means of a telescoping mast. This height was selected to emulate typical street microcell base stations mounted on existing structures such as street or traffic lights. The antenna had an omnidirectional azimuthal pattern, and a 60-, 35-, and 20-degree-elevation beamwidth for 912, 1920, and 5990 MHz, respectively.

A van was used to house and transport the transmitter equipment (Figure 1). Although the transmitter could be moved, it remained in a fixed location for the duration of the line-of-sight (LOS) and non-line-of-sight (NLOS) experiments (see Glossary of Terms) at each building. In order to ensure valid comparisons among the data collected, all data for each transmission path was collected in a single day while the transmitter remained in a fixed location. The transmitter was powered by a diesel generator which was towed behind the van. Three unmodulated waves at 912, 1920 and 5990 MHz were radiated simultaneously by one antenna. Two transmission paths were measured for each building: one for LOS and one for NLOS data collection. For

Figure 1. Photograph of van used to transport transmitter equipment.

the high-rise building measurements, the transmitting antenna was tilted to an angle of 24 degrees from horizontal. This allowed the main beam of the antenna to illuminate more floors of the building, and reduced the impact of the narrow-beamwidth antenna elevation patterns.

The three transmitted signals were generated by three frequency synthesizers. The signals were amplified and filtered separately to avoid intermodulation distortions, and combined by a quadruplexer with the unused input loaded. The combined signal was fed through a low-loss cable to the wideband, omnidirectional vertically polarized antenna. Figure 2 shows the block diagram of the transmitting equipment.

The measured input to the antenna was 15 dBm. The antenna gain was 0, 2.6, and 3.6 dBi at 912, 1920, and 5990 MHz, respectively. The effective isotropic radiated power (EIRP) from the transmitter is the sum of the input and the gain, or 15, 17.6, and 18.6 dBm at 912, 1920, and 5990 MHz, respectively.

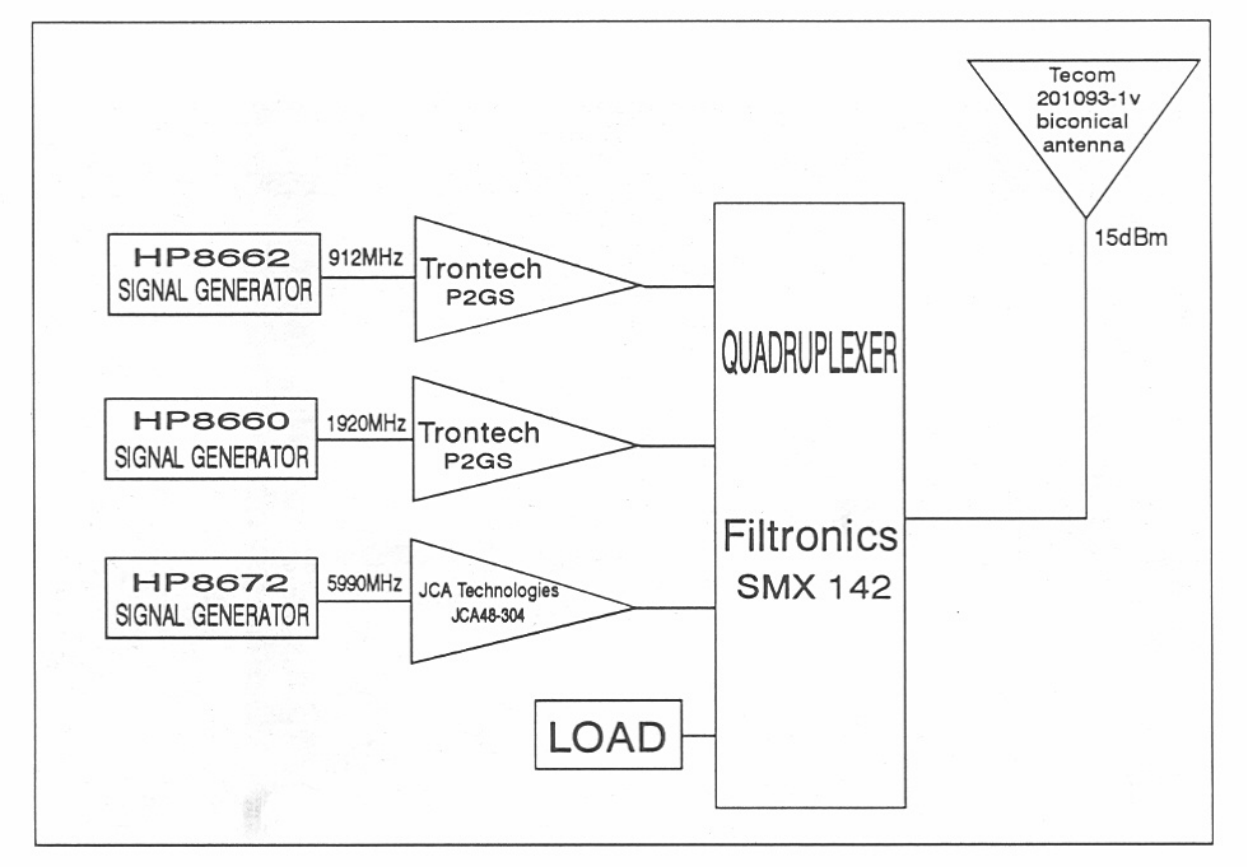

Figure 2. Block diagram of transmitter equipment.

2.1.2 Receiver

The receiver equipment, shown in Figure 3, consisted of an omnidirectional, vertically polarized antenna, identical to the transmitting antenna. The receiving antenna was manually carried through the buildings, supported by a special harness. This kept the antenna vertical, kept the antenna height constant (1.9 m), and avoided head shadowing. The received signal was divided by a quadruplexer with the unused output terminated. The active outputs of the quadruplexer were individually filtered and amplified. To decrease the noise figure of the system, the quadruplexer, filters, and low-noise amplifiers were secured to the antenna and fed through short, low-loss cables. To allow for mobility of the antenna, the signal was passed through 30 m of low-loss coaxial cables before entering three spectrum analyzers. The 5990-MHz channel included a second low-noise amplifier inserted at the input to the spectrum analyzer to

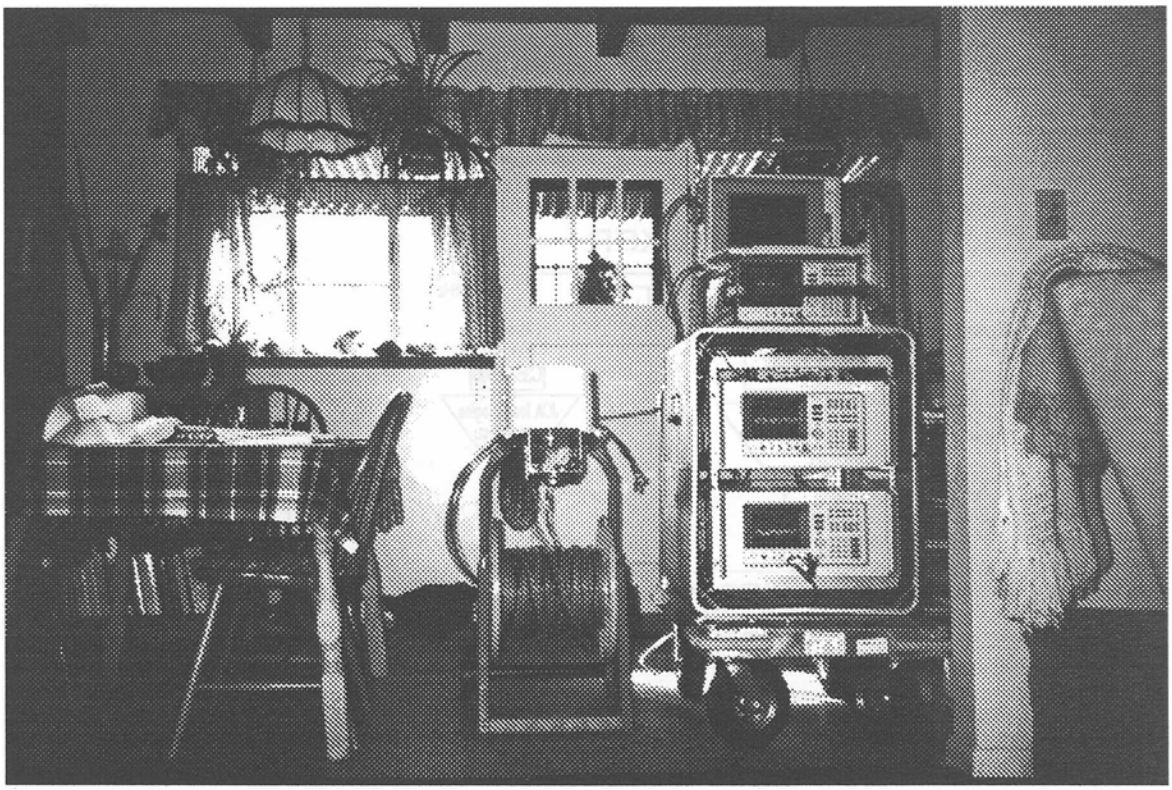

Figure 3. Photograph of receiver system.

make up for the relatively higher loss of the long coaxial cable at the higher frequency. The spectrum analyzers were controlled and the data collected automatically over a general purpose interface bus (GPIB) by a personal computer (PC). A functional block diagram of the receiver equipment is shown in Figure 4.

The measured gain of the receiver amplifiers was 26, 26, and 37 dB at 912, 1920, and 5990 MHz, respectively. The antenna gain was 0, 2.6, and 3.6 dBi at 912, 1920, and 5990 MHz, respectively. The calculated gain of the receiver relative to isotropic gain is the sum of the antenna gain and the receiver amplifier gain, or 26, 28.6, and 40.6 dB at 912, 1920, and 5990 MHz, respectively.

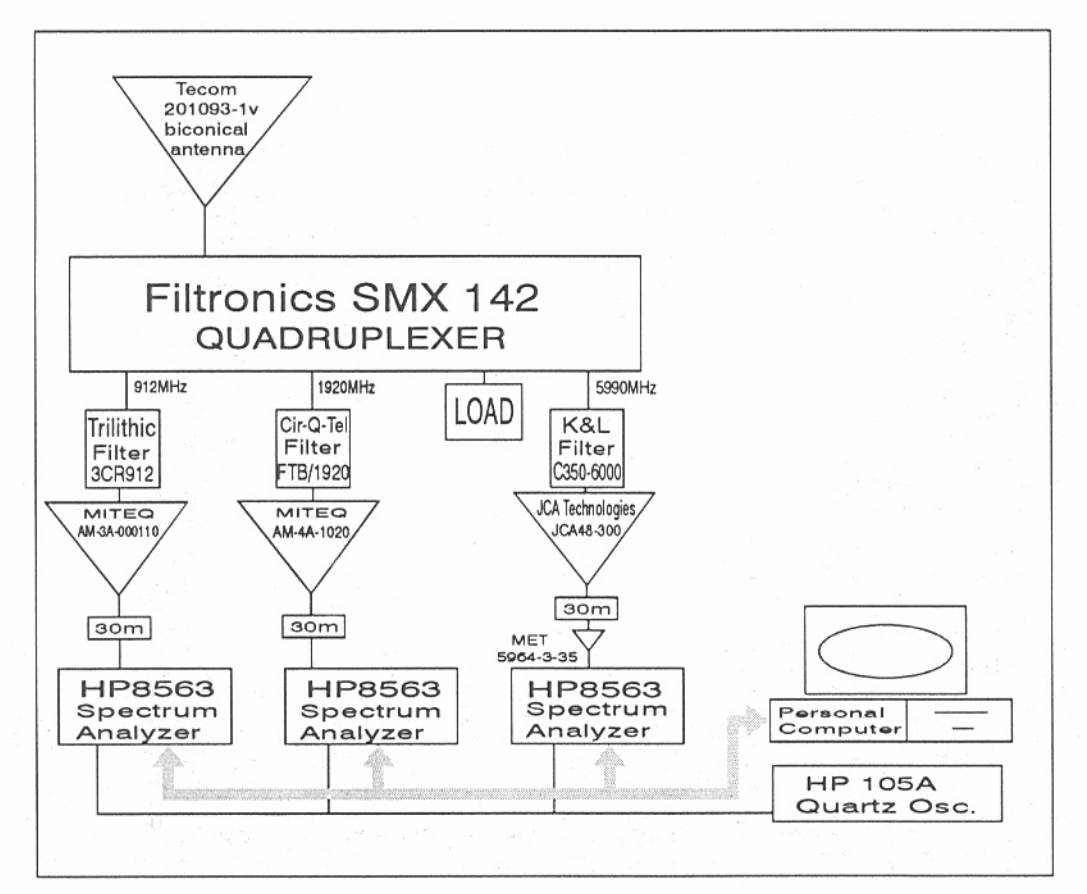

Figure 4. Block diagram of receiver equipment.

2.2 Calibration and Measurement Procedure

The transmitter was calibrated every morning (after allowing adequate time for the system to reach operating temperature) with a spectrum analyzer to ensure that all frequencies produced 15 dBm at the input to the antenna. The receiver was calibrated with a noise diode every morning and every afternoon. All spectrum analyzers were self-calibrated before measurements were taken in each room.

Although precise distance measurements were not required, a precision electronic distance meter (EDM) was used as the easiest means of gathering distance information. All distance measurements reported here are approximations within 10 m.

Reference measurements (see Glossary of Terms) were made at ground level outside each building, one for each transmission path. To avoid the possibility of measuring a deep fade caused by multipath as the reference, a zig-zag pattern with a radius greater than the longest transmitted wavelength was traversed along outside walls of each building. A minimum sample of 100 wavelengths was collected for each reference.

Within the buildings, the measurements were made by moving the receiving antenna in a zig-zag pattern through the area measured. This pattern was used to ensure that the entire area was covered, not just the perimeter. In the residential measurements, a zig-zag pattern was traversed across the full area of each room. Five representative rooms were measured to acquire an average for each residential building. For the high-rise building measurements, a zig-zag pattern was traversed across each of the four corners (except in instances where we were denied access to the area) on representative floors, covering an area of approximately 40 m^2 per corner.

In each room measured, a zig-zag pattern with each leg greater than the maximum transmitted wavelength (0.66 m) was traversed. To avoid aliasing, we collected four samples per the shortest wavelength (0.05 m), or 80 samples per meter. A sampling rate of 60 Hz (601 samples in a 10-s sweep) was set by the spectrum analyzer, and the speed of the receiver was 0.75 m/s. Taking samples of at least 100 wavelengths per room gave us a minimum data collection time of 41 s. By collecting 5 sweeps of the spectrum analyzer, we collected a minimum of 3000 samples or 750 wavelengths per room. Thus we could observe the fast and slow fading effects, and deep fades (30 dB) at the shortest wavelength.

2.3 Data Format

The data were stored in ASCII format on the hard disk of a PC, and downloaded to floppy disk daily. Since five 10-s sweeps were taken in each room or corner, five files were generated. Each file contained data from all three frequencies. The equipment was then moved to the next room or corner, and the process was repeated. Because the signals were received by spectrum analyzers, real-time data were viewed as they were collected. This allowed the measurements to be checked immediately and retaken if erroneous.

3. MEASUREMENT LOCATIONS

3.1 Residential Building Information

We took measurements at seven private residences in and around Boulder, Colorado. Data were taken on the main floor, as well as in the basements and on second floors, when present. Figures 5 through 11 show the LOS and NLOS paths, and neighborhood layouts for each residence. In these figures, "TX" refers to the transmitter locations, and "RX" refers to the receiver location. Appendix A contains path loss and building layout information for all residential measurements.

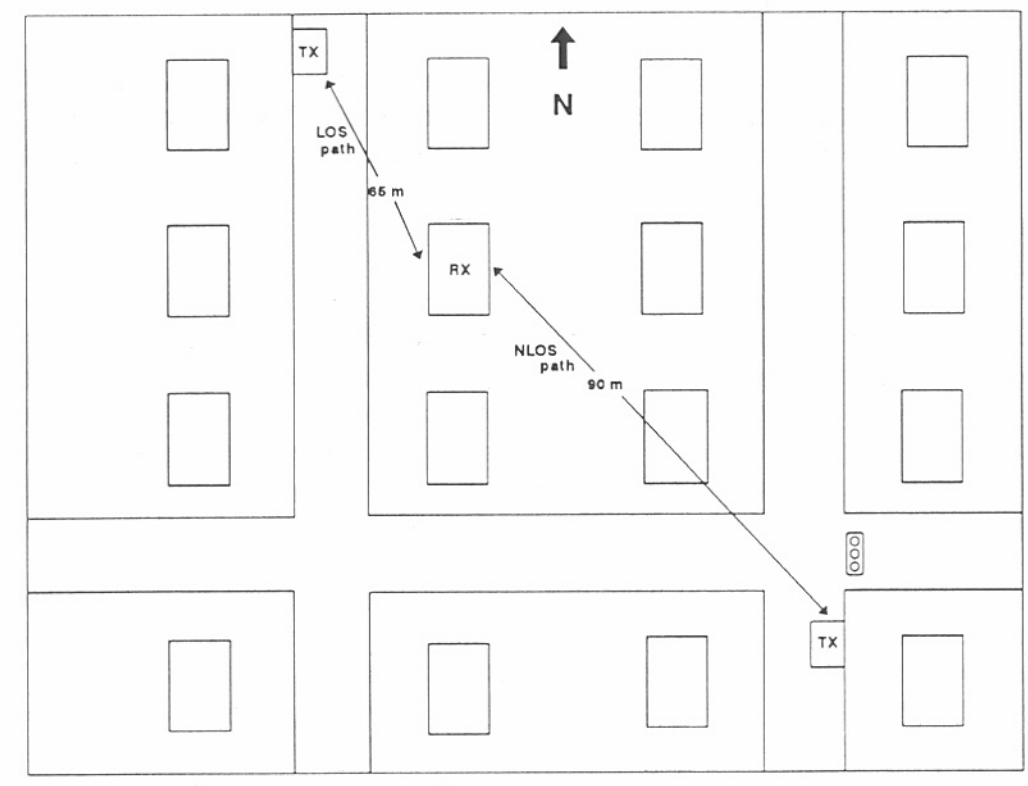

Figure 5. Diagram of residence-1 neighborhood (not to scale).

Residence 1 was a single-story brick, wire mesh, and plaster house. The closest street contained fewer then ten parked cars, and fewer than ten cars passed by per hour. The surrounding streets contained single-story houses, with approximately 800 m^2 of land each. In front of the house were two 15-m pine trees. The basement was completely underground with small window wells. For the LOS measurements, the transmitter was located 65 m northwest of the building. For the NLOS measurements, the transmitter was located 90 m southeast of the building.

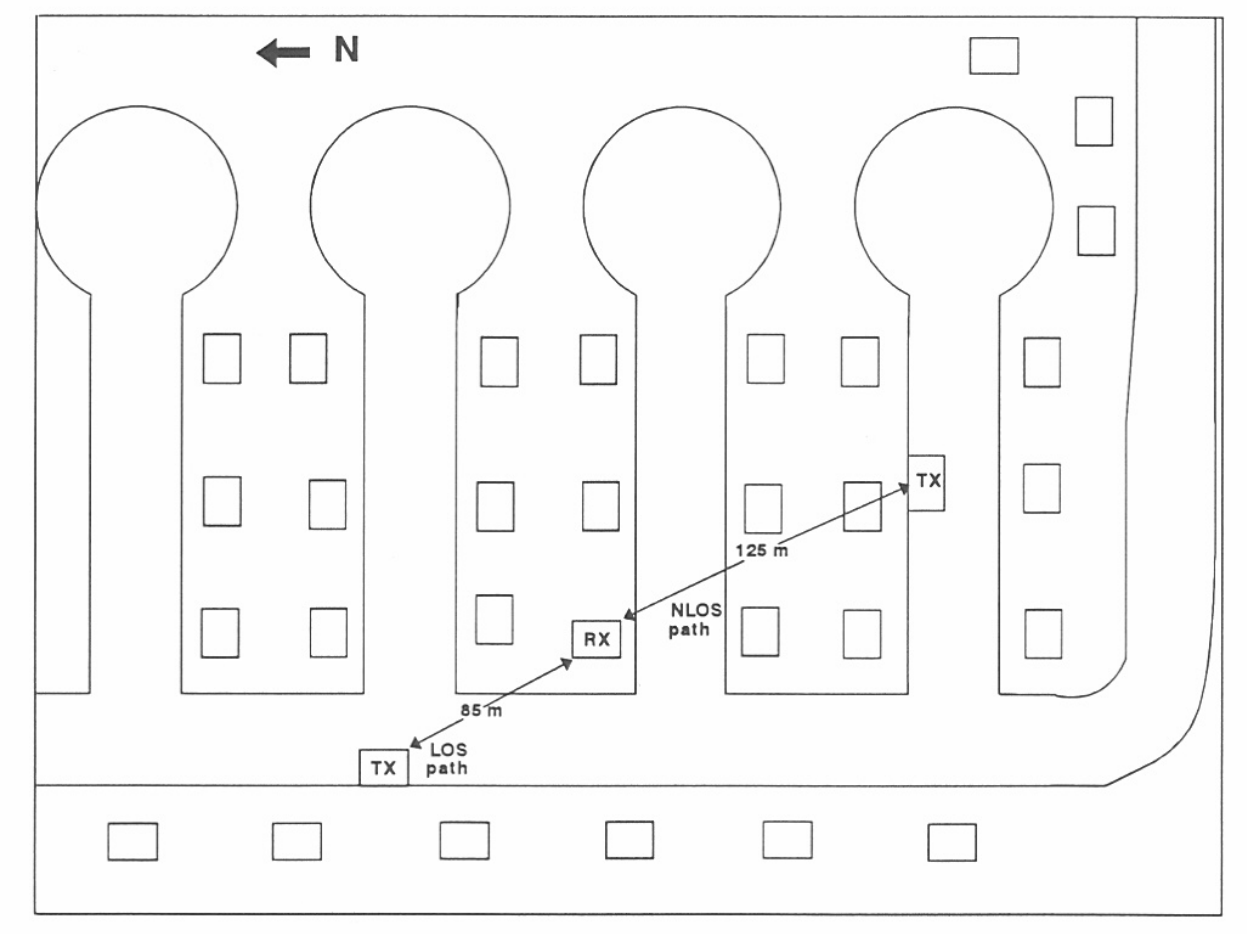

Figure 6. Diagram of residence-2 neighborhood (not to scale).

Residence 2 was a tri-level, brick veneer and wood building located on a street with fewer than ten cars passing per hour and no parked cars. The surrounding streets contained one- and two-story houses, with approximately 1200 m^2 of land per house. There were two 15-m tall pine trees located on the northwest side of the house. The basement was half underground and had large, above ground windows. For the LOS measurements, the transmitter was located 85 m northwest of the building. For the NLOS measurements, the transmitter was located 125 m southeast of the building.

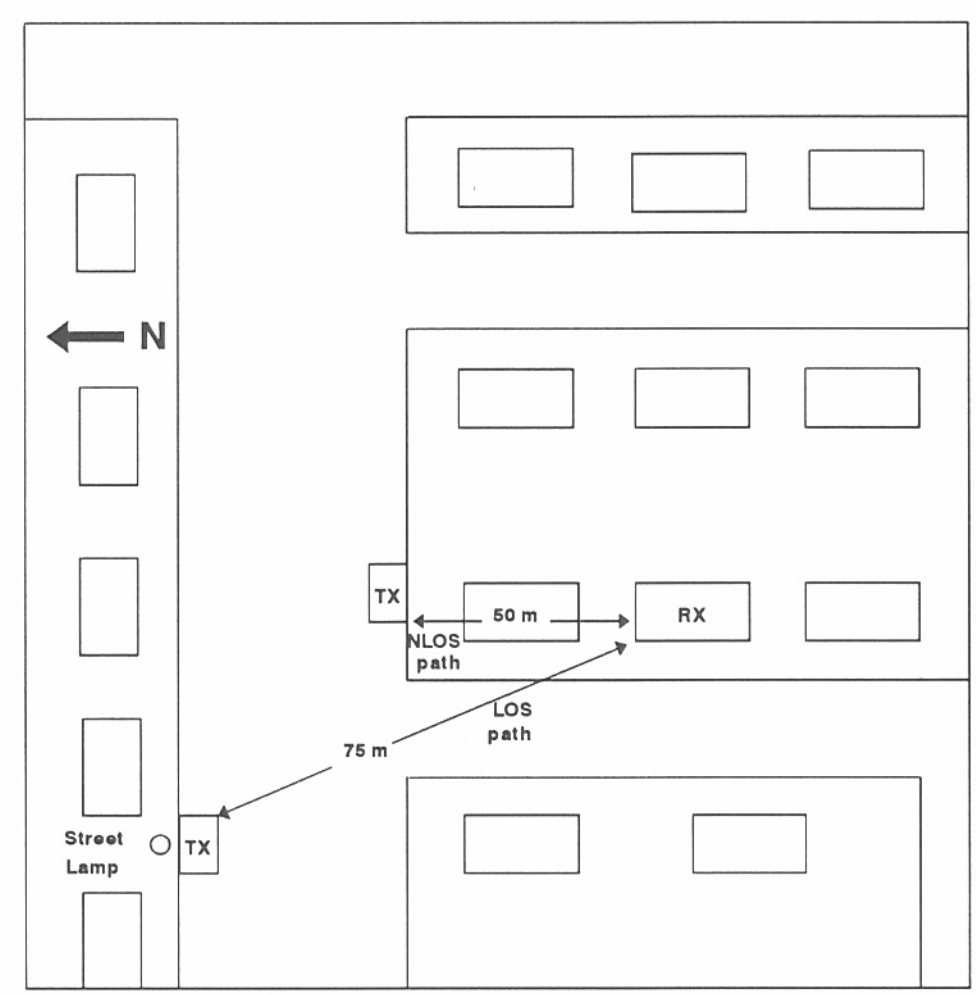

Figure 7. Diagram of residence-3 neighborhood (not to scale).

Residence 3 was a single-story, brick veneer building located on a street with fewer than ten passing cars per hour and no parked cars. The surrounding streets contained one- and two-story houses, with approximately 1200 m^2 of land per house. There was one 8-m tall bare tree and some 1-m tall evergreen shrubs around the house. The basement was completely underground and had small window wells. For the LOS measurements, the transmitter was located 75 m northwest of the building. For the NLOS measurements, the transmitter was located 50 m north of the building.

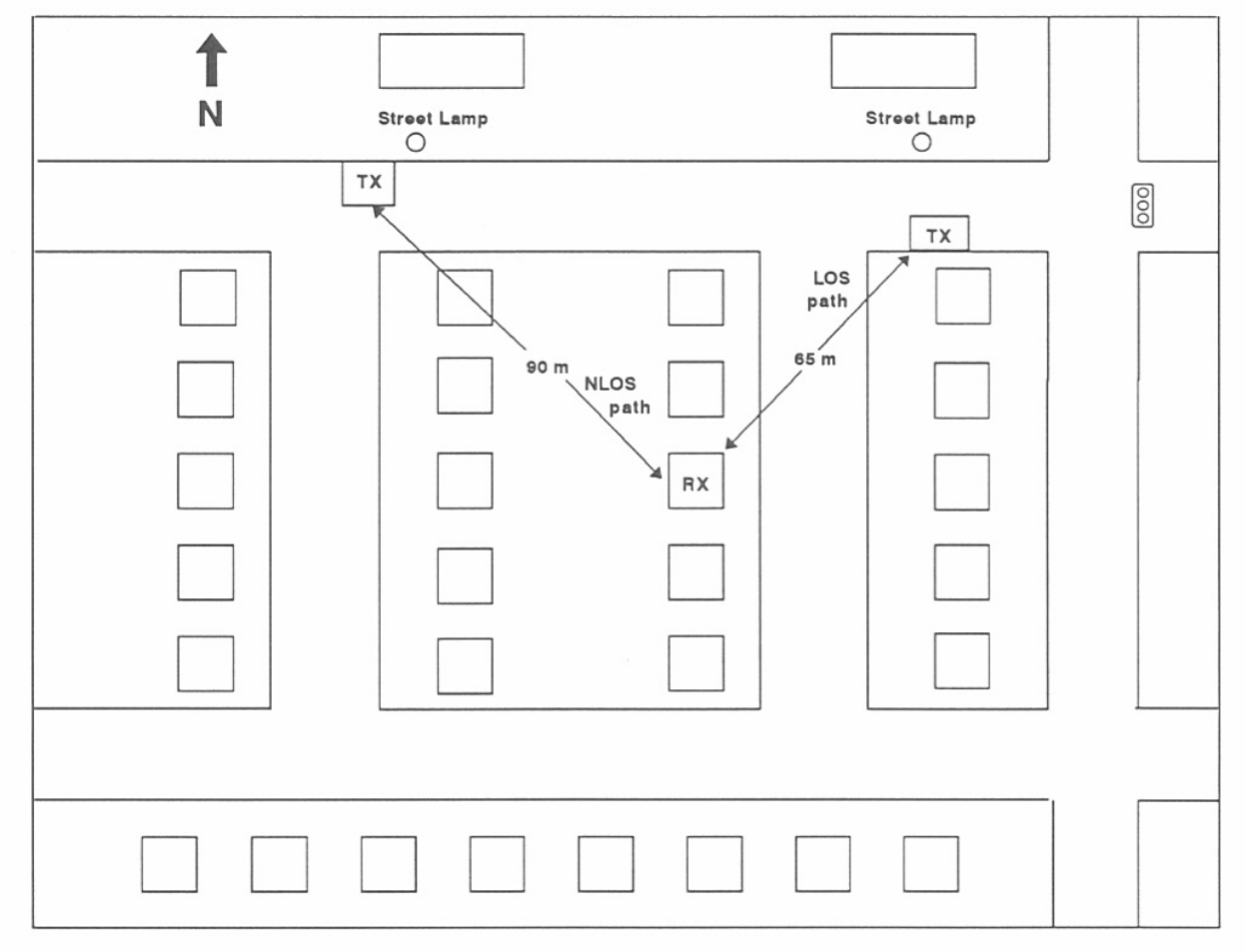

Figure 8. Diagram of residence-4 neighborhood (not to scale).

Residence 4 was a tri-level, brick building located on a street with fewer than 20 cars passing per hour. There were more than ten cars parked along the street near the house. The streets contained one- and two-story houses, with approximately 800 m^2 of land per house. The basement was half underground with large windows. For the LOS measurements, the transmitter was located 65 m northeast of the building. For the NLOS measurements, the transmitter was located 90 m northwest of the building.

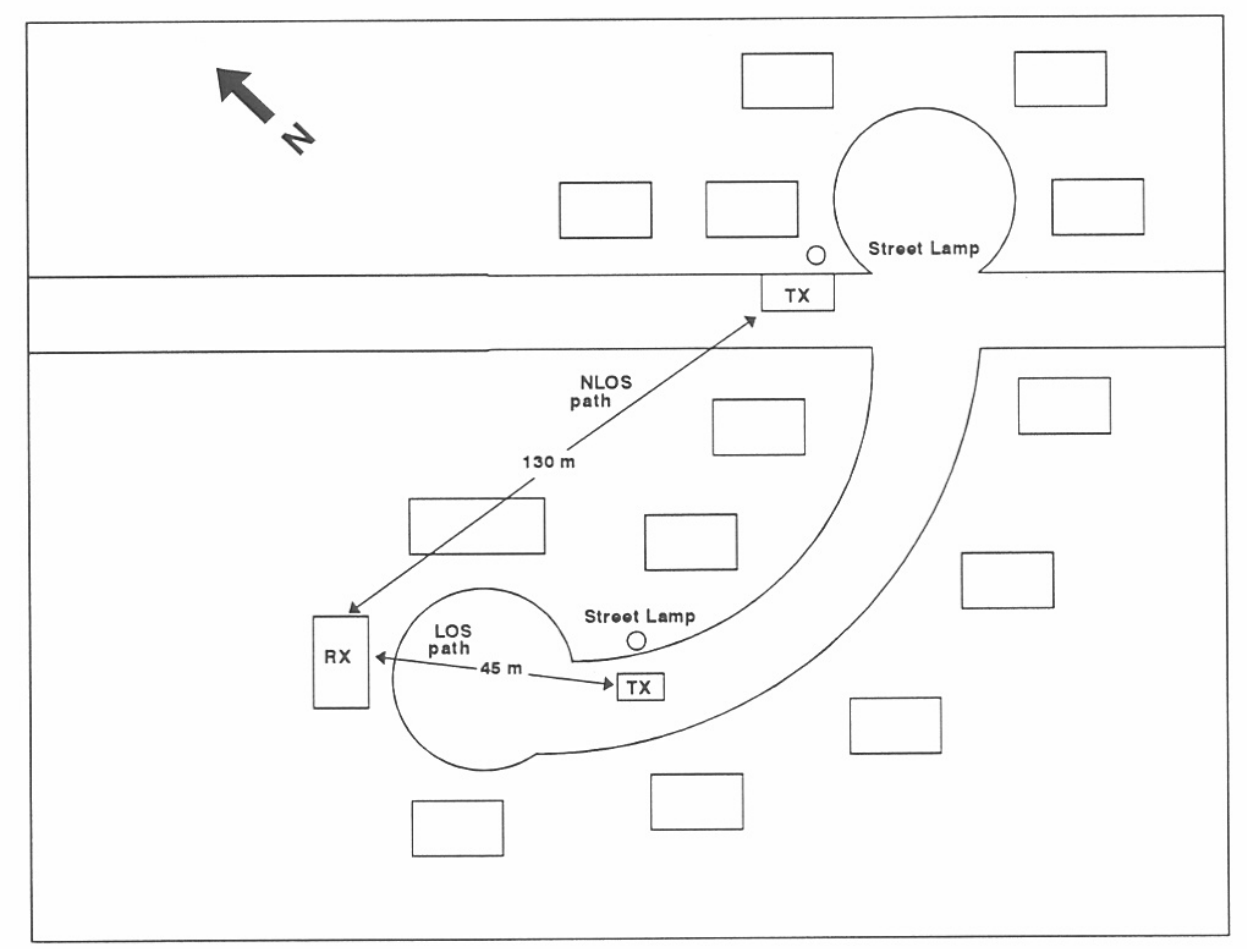

Figure 9. Diagram of residence-5 neighborhood (not to scale).

Residence 5 was a large, two-story, wood and brick veneer building with Thermoply® reflective insulation. It was located on a cul-de-sac with fewer than five cars passing per hour, and no cars parked on the street. The street contained large two-story houses, approximately 2000 m^2 of land per house, and no vegetation. The basement was completely underground and had large window wells. For the LOS measurements, the transmitter was located 45 m southeast of the building. For the NLOS measurements, the transmitter was located 130 m east of the building.

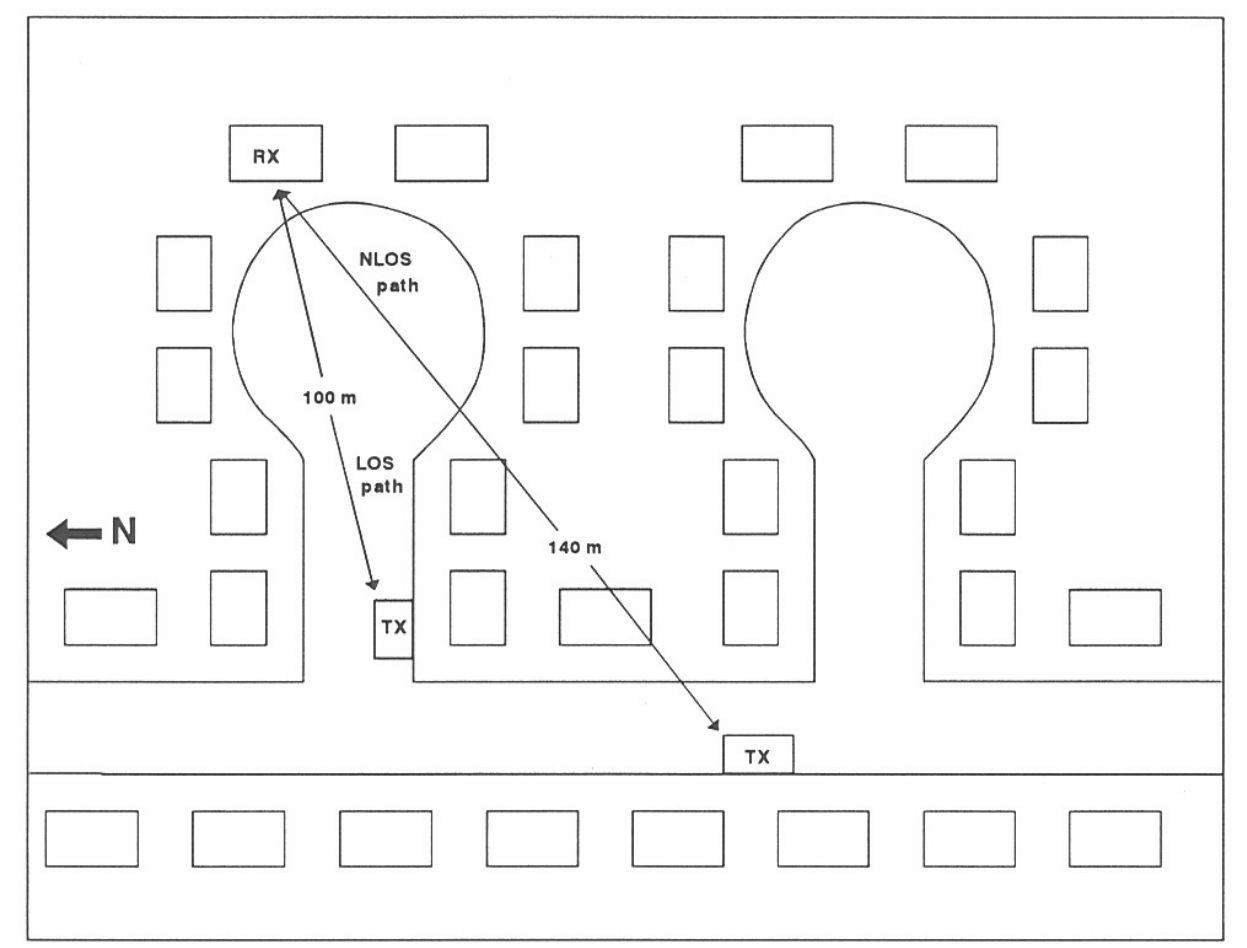

Figure 10. Diagram of residence-6 neighborhood (not to scale).

Residence 6 was a two-story, aluminum and brick veneer building located on a street with fewer than five cars passing per hour and fewer than five cars parked on the street. The street contained one- and two-story houses, with approximately 1000 m^2 of land per house. The basement was completely underground and had small window wells. For the LOS measurements, the transmitter was located 100 m southwest of the building. For the NLOS measurements, the transmitter was located 140 m southwest of the building.

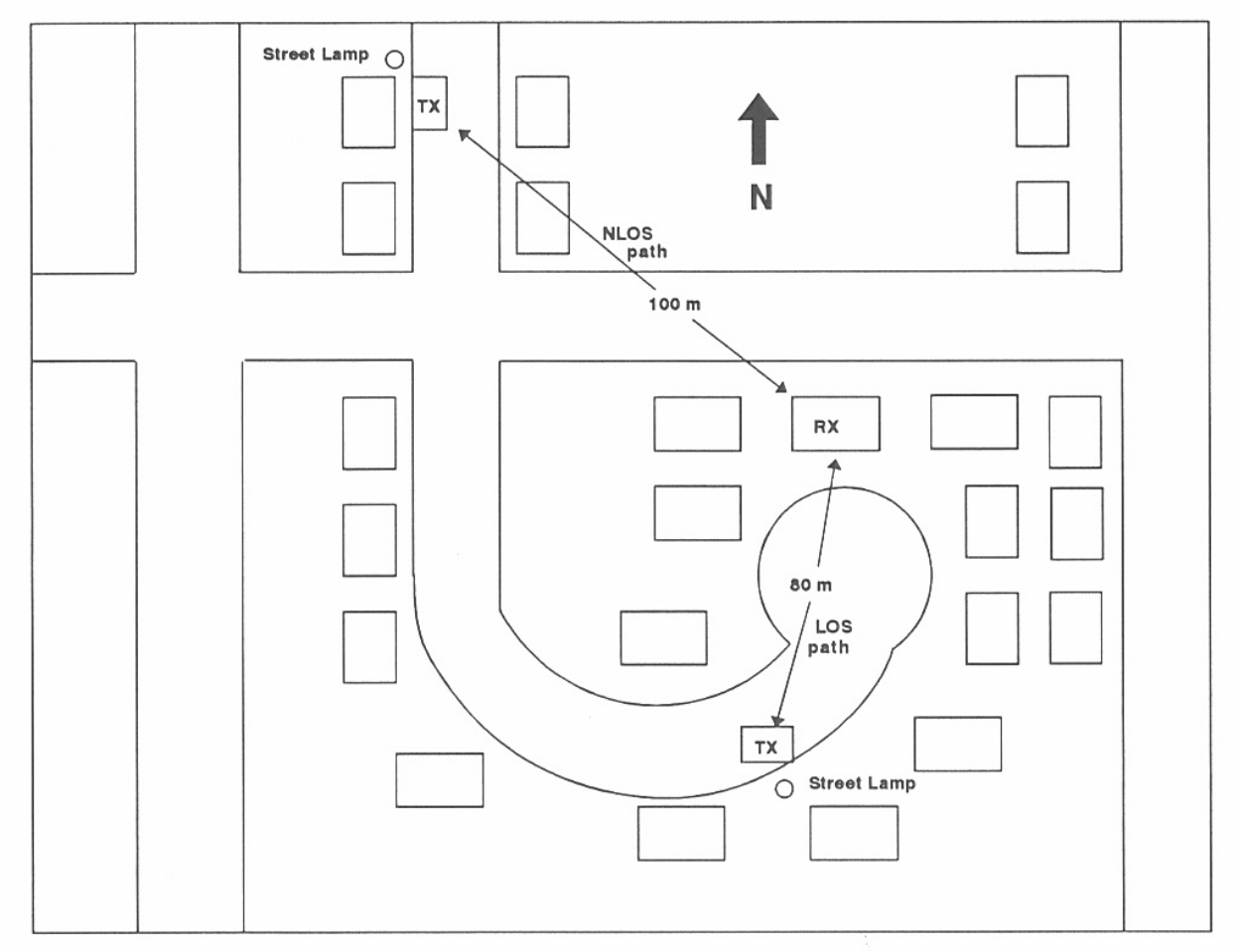

Figure 11. Diagram of residence-7 neighborhood (not to scale).

Residence 7 was a two-story, wood and brick veneer building located on a street with fewer than ten cars passing per hour. The surrounding streets contained one- and two-story houses, with approximately 800 m^2 of land per house. The basement was completely underground and had large window wells. For the LOS measurements, the transmitter was located 80 m south of the building. For the NLOS measurements, the transmitter was located 100 m northwest of the building.

3.2 High-rise Building Information

We took measurements in four high-rise buildings in downtown Denver, Colorado (Figures 13 through 16). This area consisted of closely spaced buildings with heights typically ranging from 3 to 30 stories. A diagram of the environment, with the total number of floors listed for each building, is shown in Figure 12. Due to logistical considerations, the transmitter was not parked under street lamps or traffic lights, but was parked to ensure appropriate transmission paths. For all high-rise buildings measured, the surrounding streets contained more than 20 parked cars, and more than 200 vehicles and 50 pedestrians passed per hour. The interiors of the high-rise buildings had an open-face layout with soft, low, cubicle-wall partitions. Appendix B contains the path loss data for each high-rise building measured.

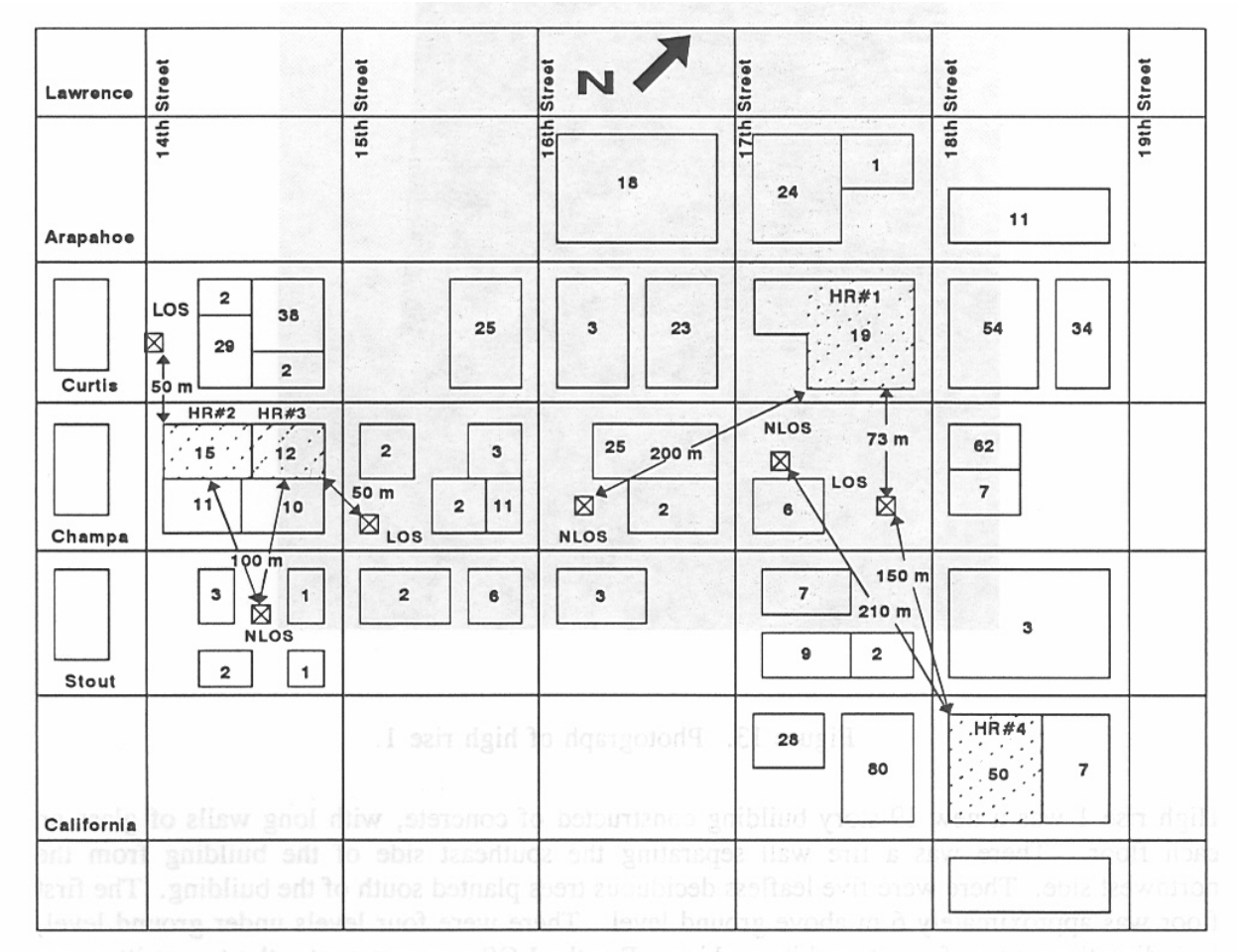

Figure 12. Area studied in Denver, Colorado. (Numbers indicate the number of stories for each building shown; not to scale.)

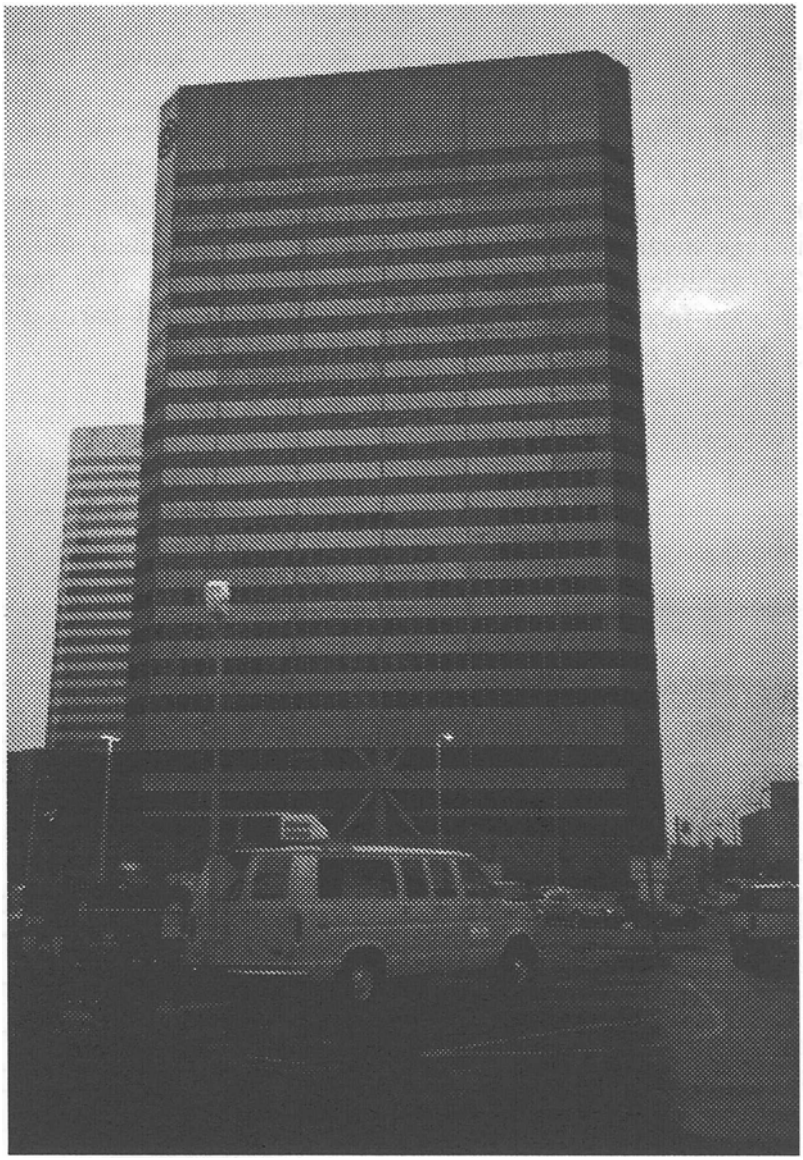

Figure 13. Photograph of high rise 1.

High rise 1 was a new 19-story building constructed of concrete, with long walls of glass on each floor. There was a fire wall separating the southeast side of the building from the northwest side. There were five leafless deciduous trees planted south of the building. The first floor was approximately 6 m above ground level. There were four levels under ground level, including three areas for automobile parking. For the LOS measurements, the transmitter was located 70 m southeast of the building. For the NLOS measurements, the transmitter was located 200 m southwest of the building.

Figure 14. Photograph of high rise 2.

High rise 2 was a 65-year-old, 15-story, stone building with many windows evenly spaced throughout the building. There were two leafless deciduous trees to the northwest of the building. For the LOS measurements, the transmitter was located 50 m northwest of the building. Because of the layout of the city, only the west and south corners of the building were line-of-sight to the transmitter and were measured. For the NLOS measurements, the transmitter was located 100 m southeast of the building.

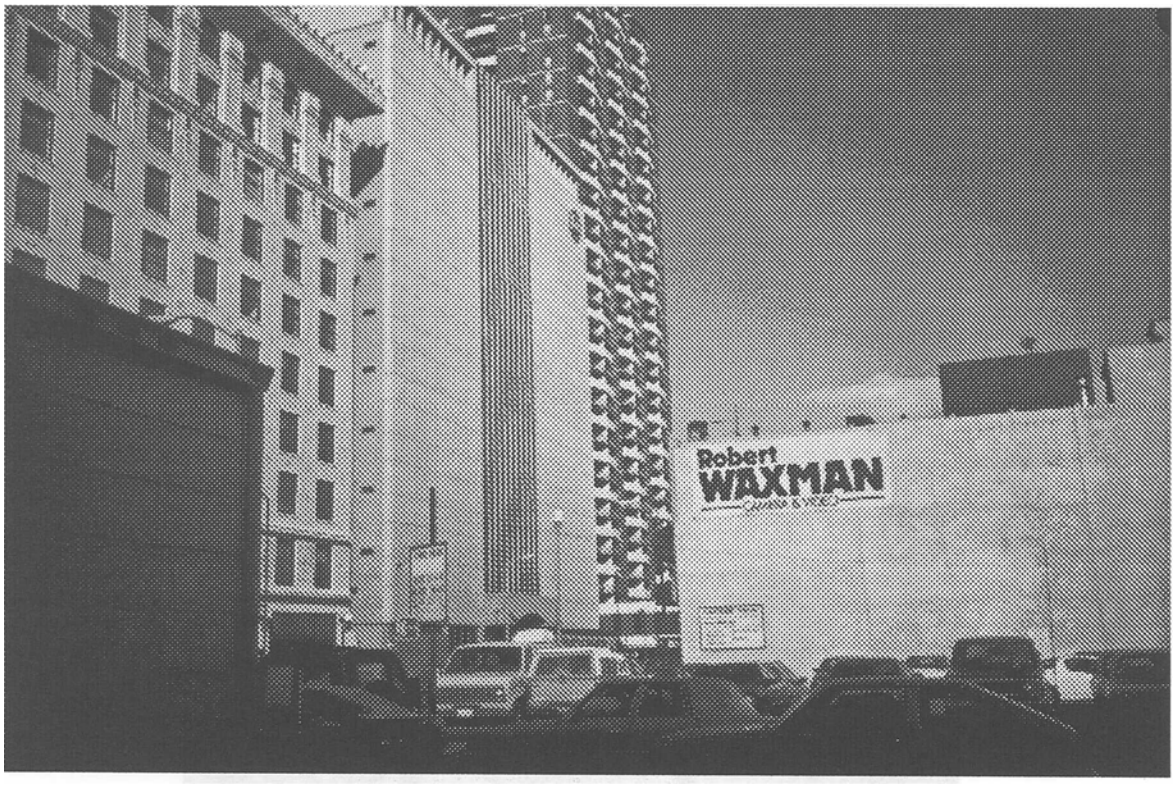

Figure 15. Photograph of high rise 3.

High rise 3 was a 12-floor, stone building with a column of windows running down the center of two sides of the building. It comprised one quarter of the block. There was no surrounding foliage. For the LOS measurements, the transmitter was located 50 m east of the building. Due to the layout of this block, only the east and north corners were line-of-sight to the transmitter and were measured. For the NLOS measurements, the transmitter was located 100 m southeast of the building.

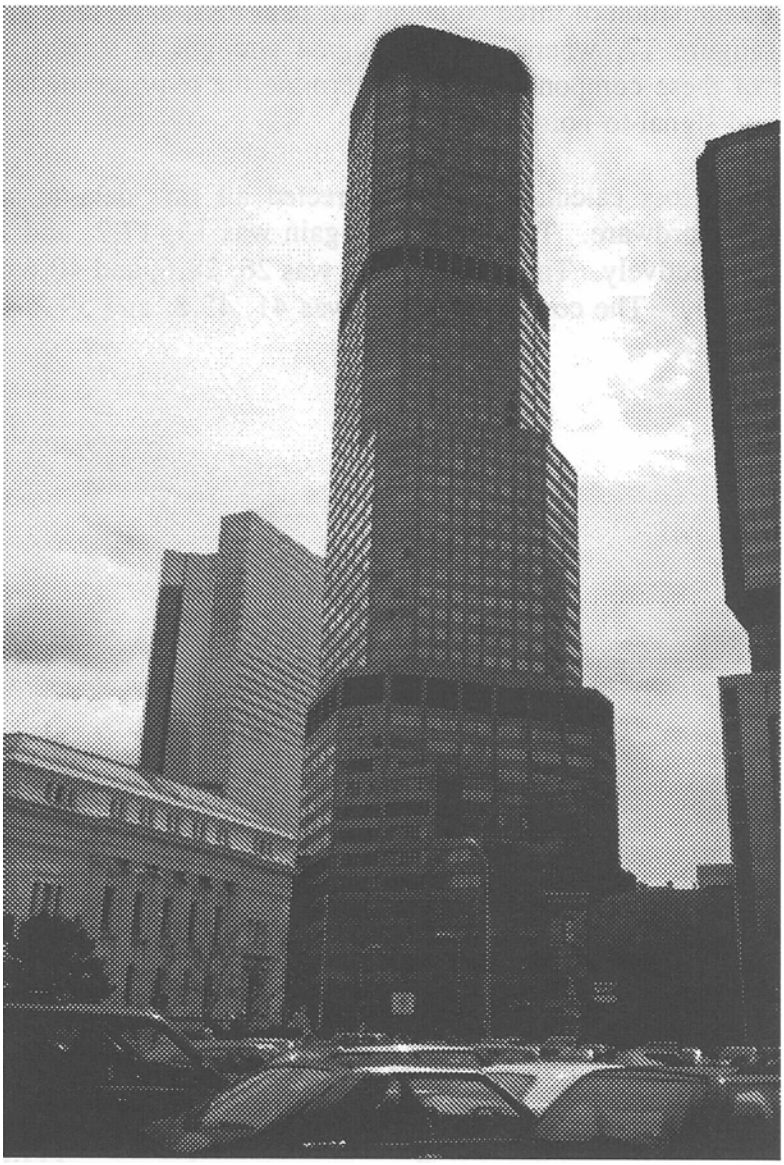

Figure 16. Photograph of high rise 4.

High rise 4 was a new 50-story building, which varied in shape as the floor levels increased. It was constructed of concrete and had many windows evenly distributed throughout the building. There was no surrounding foliage. For the LOS measurements, the transmitter was located 150 m northwest of the building. For the NLOS measurements, the transmitter was located 210 m northwest of the building.

4. DATA ANALYSIS

For point-to-multipoint communication environments, narrowband propagation characteristics can be described as a combination of three components: path loss, slow fading, and fast fading. This is illustrated in Figure 17, where received signal strength is shown as a function of distance. Knowledge of these components helps determine the required distance between cell sites, handoff speed, and signal-to-noise ratio.

Before initiating any path loss calculations, we corrected all raw data to subtract the gain introduced by the system hardware. The transmitter gain was 15, 17.2, and 18.6 dBi at 912, 1920, and 5990 MHz, respectively. The receiver gain was 26, 28.6, and 40.6 dB at 912, 1920, and 5990 MHz, respectively. The correction factor was 41, 45.8, and 59.2 dB at 912, 1920, and 5990 MHz, respectively.

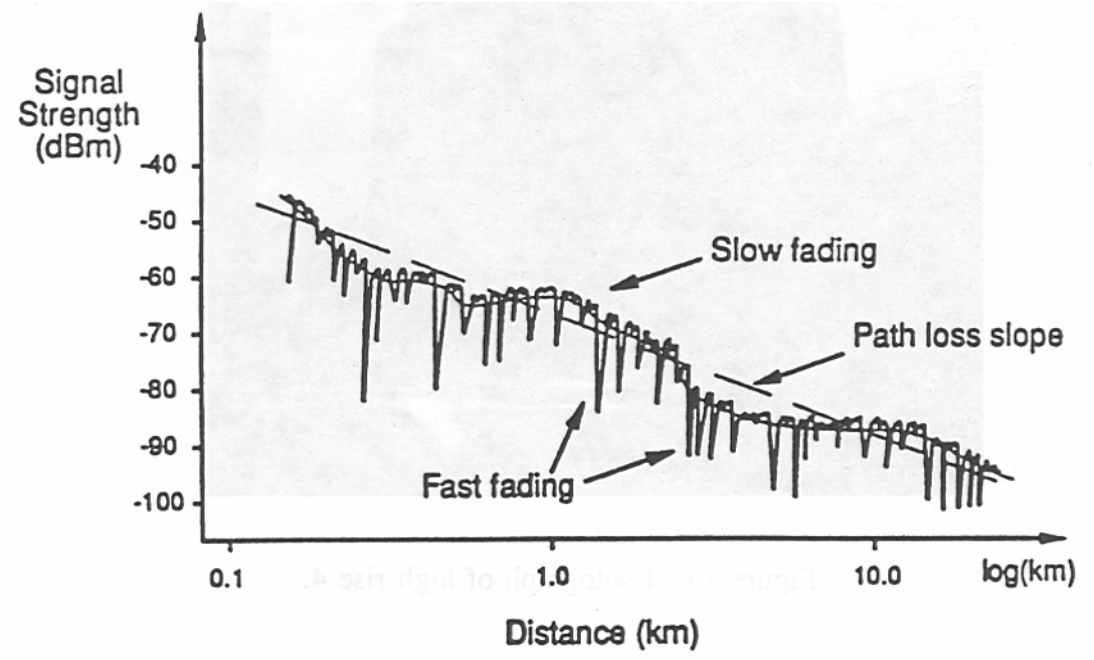

Figure 17. Characteristics of narrowband fading [2]. This graph is intended for use in this report to illustrated fading characteristics. Some data points may have been omitted for clarity.

4.1 Path Loss Calculations

As the distance separating a transmitter and receiver increases, the received signal strength tends to decrease due to wave spreading. This type of attenuation is known as path loss (see Glossary of Terms). Knowledge of the amount of path loss expected is critical in determining cell sizes for optimum performance of PCS systems.

The theoretical path loss, L_T, in decibels can be expressed mathematically as

$$L_T = L + X \log(d), \tag{1}$$

where L is a loss constant which includes antenna gain,
X is the attenuation factor (dB/decade), and
d is the distance between transmitter and receiver.

In free space, the attenuation factor is 20 dB/decade. We expect this value to be larger in building penetration measurements.

The experimental median (see Glossary of Terms) path loss, L_M, in decibels between the transmitter and receiver can be calculated from the measured data using the formula

$$L_M = P_{RX} - P_{RX\_ideal}, \tag{2}$$

where P_{RX} is the median measured power at the receiver (dBm), and
P_{RX_ideal} is the ideal received power (dBm).

Median measured path loss for all residential and high-rise buildings is shown in Appendix A and Appendix B, respectively. Path loss versus distance plots are shown in Figures 18 through 20. These plots include all buildings and transmission paths measured. Each data point represents the median path loss per building and the average horizontal distance between transmitter and receiver.

Appendix C shows the path loss distribution for a selection of rooms in the residential buildings, and floors of the high-rise buildings. These histograms show uni-modal and bi-modal distributions.

4.1.1 Breakpoint

There is a phenomenon referred to as the path loss breakpoint [3,4,5]. It consists of a change in path loss slope at some radial distance from the transmitter. It is caused by the reflection of the transmitted signal by the ground. This multipath signal interferes with the direct path signal and usually occurs only in areas with clear LOS and ground reflection paths. Theoretically, the path loss should decrease 20 dB/decade close to the transmitter, and decrease 40 dB/decade after

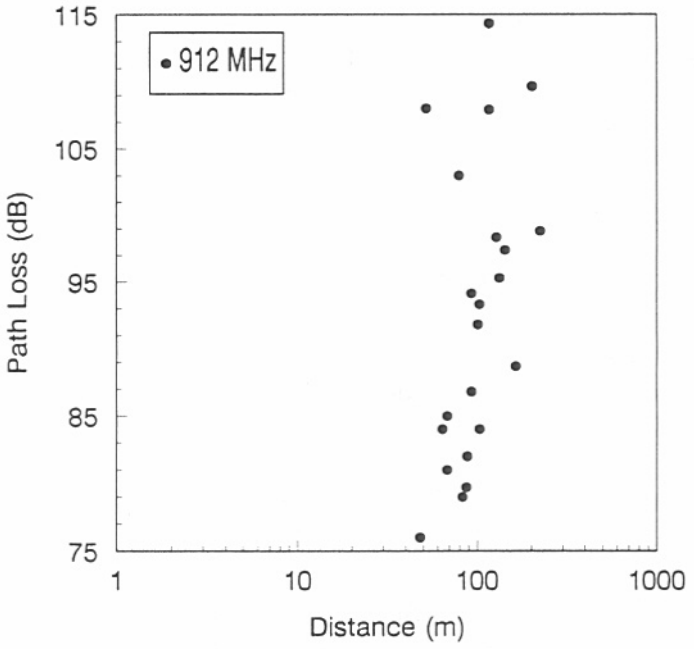

Figure 18. Path loss versus distance at 912 MHz.

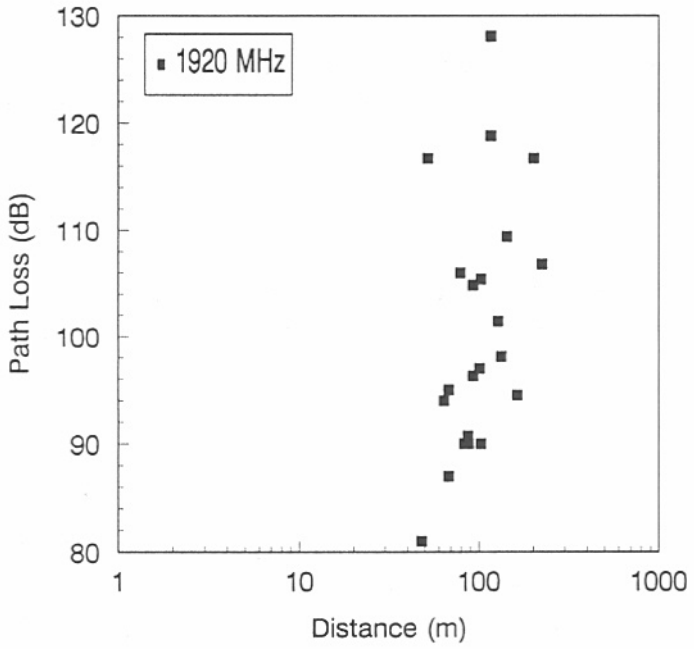

Figure 19. Path loss versus distance at 1920 MHz.

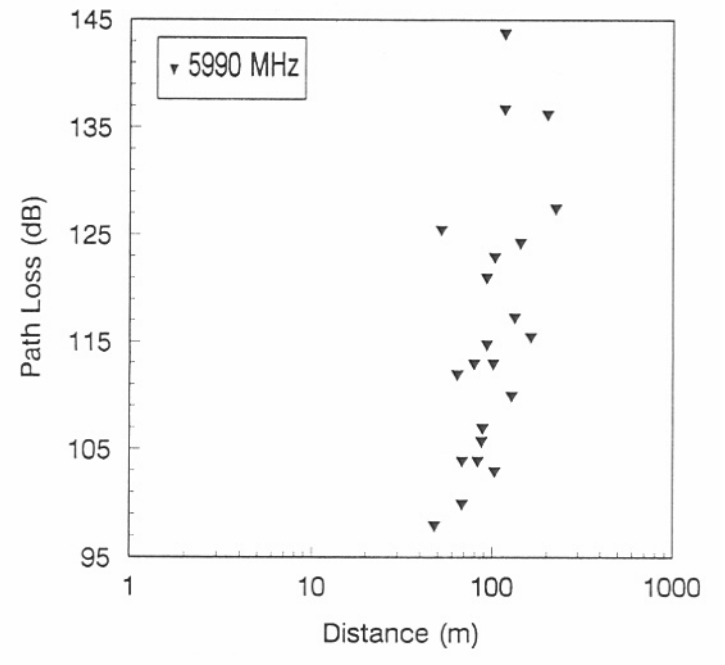

Figure 20. Path loss versus distance at 5990 MHz.

the path loss breakpoint occurs. (Note: this phenomenon helps to increase spectrum efficiency by allowing for increased frequency reuse at distances larger than the breakpoint.)
The breakpoint radius from the transmitter, R_b, can be calculated using the formula

$$R_b = \frac{2h_t h_r}{\lambda}, \tag{3}$$

where h_t is the height of the transmitting antenna,
h_r is the height of the receiving antenna, and
λ is the wavelength, all in the same units [6].

The expected breakpoint radii for our data are given in Table 1. Since our measurements were taken for microcells, we do not have a wide range of distance data. This makes it more difficult to determine a breakpoint. Also, the more obstacles and terrain changes between the transmitter and receiver, the less likely it becomes that a breakpoint will be seen [6]. Since half of our data was non-line-of-sight, half of the data points are likely to show no breakpoint. For the 5990-MHz data, we do not expect to see a breakpoint because all our measurements were taken at less than the calculated breakpoint radius of 400 m. For the data presented in this paper, no breakpoints were determined.

Table 1. Expected Breakpoint Radii

Frequency (MHz)	R_b (m)
912	60
1920	130
5990	400

4.1.2 Difference in Received Signal Strength

Received signal strength is an important parameter in telecommunications because it indicates the amount of transmitter power necessary to obtain coverage in an area. Received signal strength is calculated using the free space formula

$$P_r = P_t G_r G_t \frac{\lambda^2}{(4\pi r)^2}, \tag{4}$$

where $\boldsymbol{P_r}$ is the received power,
$\boldsymbol{P_t}$ is the transmitted power,
$\boldsymbol{G_r}$ is the gain of the receiving antenna,
$\boldsymbol{G_t}$ is the gain of the receiving antenna, and
$\boldsymbol{r}$ is the distance between transmitter and receiver.

The antenna gains are calculated using the formula

$$G = A_e \frac{4\pi}{\lambda^2}, \tag{5}$$

where $\boldsymbol{A_e}$ is the effective aperture of the antenna and
$\boldsymbol{G}$ is the antenna gain.

Since all variables except the frequency are held constant in our application, the theoretical change in received signal strength (power) due to the change in frequency transmitted is determined by

$$\Delta P_r = 20\log(f_2 / f_1)., \tag{6}$$

The expected and measured differences between the frequencies are given in Table 2. The measured differences vary from the calculated values quite significantly. This variance is well-established by our measurements, being observed in both urban and suburban environments. These findings concur with other research findings, where differences in received signal strength of up to 4 dB (1922/880 MHz) greater than theory were found [5,7,8,9].

Table 2. Received Signal Strength Differences Between Frequencies

	1920/912 MHz (dB)	5990/1920 MHz (dB)
Theoretical	6.5	9.9
Measured Residential	7.4	12.7
Measured High Rise	10.0	22.3

4.2 Penetration Loss Calculations

The difference in signal level between the received (corrected) signal level inside the building and the reference signal level (at ground level) is defined as the building penetration loss. The building penetration loss is calculated as

$$P_{ref} - P_{rm/cnr}, \tag{7}$$

where P_{ref} is the median reference signal strength, in dBm, and
$P_{rm/cnr}$ is the median of the signal strength in a particular room or corner of a building, in dBm.

We calculated building penetration losses for each building, at each frequency, and for each transmission path separately. The total mean (see Glossary of Terms) building penetration loss was found by calculating the mean of all residential or high rise medians. Standard deviations, σ, were calculated using the formula

$$\sigma = \sqrt{\sum_{i=1}^{n} \frac{(x_i - \bar{x})^2}{n-1}}, \tag{8}$$

where x_i is the ith data point,
$\bar{x}$ is the room or corner mean, and
n is the number of data points.

Appendix D contains tables of penetration losses for each building individually. The mean NLOS residential and high-rise building penetration losses are summarized in Table 3. The mean building penetration values for both LOS and NLOS are summarized in Table 4, where "All buildings" refers to the average of the high rise and residential measurements.

Table 3. Mean NLOS Penetration Losses

Building	912 MHz (dB)	1920 MHz (dB)	5990 MHz (dB)
Residential	7.7	11.6	16.1
High Rise	12.5	15.5	20.0

Table 4. Mean Penetration Losses for Both Transmission Paths

Frequency	Building	Loss (dB)
912 MHz	Residential	6.4
	High Rise	11.2
	All Buildings	8.2
1920 MHz	Residential	8.4
	High Rise	11.9
	All Buildings	9.8
5990 MHz	Residential	11.7
	High Rise	20.0
	All Buildings	14.1

We took NLOS and LOS measurements in each high-rise building. Time and accessibility restrictions made it impossible to measure all floors of all buildings. Receiver field strength deterioration at higher floor levels (due to distance and antenna pattern restrictions) made it impossible for us to measure floors above the fifteenth. Efforts were made to measure the same floors in each high-rise building in order to accommodate comparisons between the buildings.

The cumulative probability distribution/function (CDF) shows the probability that penetration loss is less than or equal to the value of the penetration loss shown on the abscissa of the same graph. Figures 21 and 22 illustrate the CDFs for all seven residences and four high rises, respectively. Comparing the CDF's from all three frequencies, we see that, for both environments, the higher frequencies suffer greater penetration loss for NLOS paths. This is true consistently except in the high-rise buildings where the 1920-MHz probability is greater than the 912-MHz probability at small penetration losses (less than 12 dB) and less than the 5990-MHz probability at large penetration losses (greater than 40 dB).

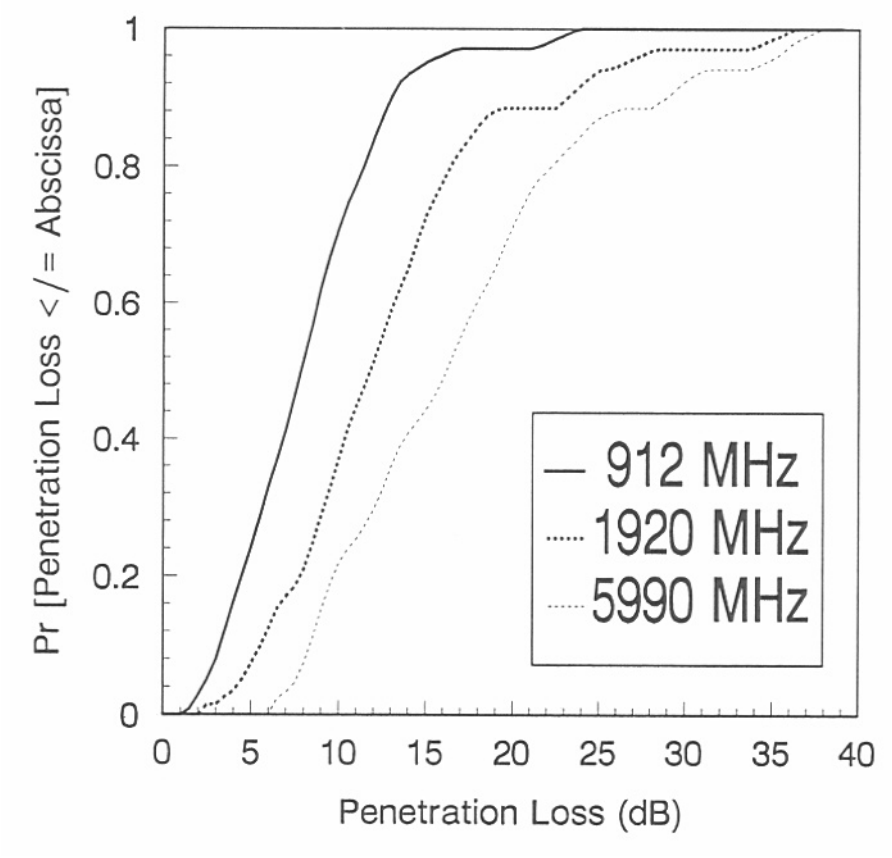

Figure 21. Cumulative probability distribution functions for NLOS residential penetration loss.

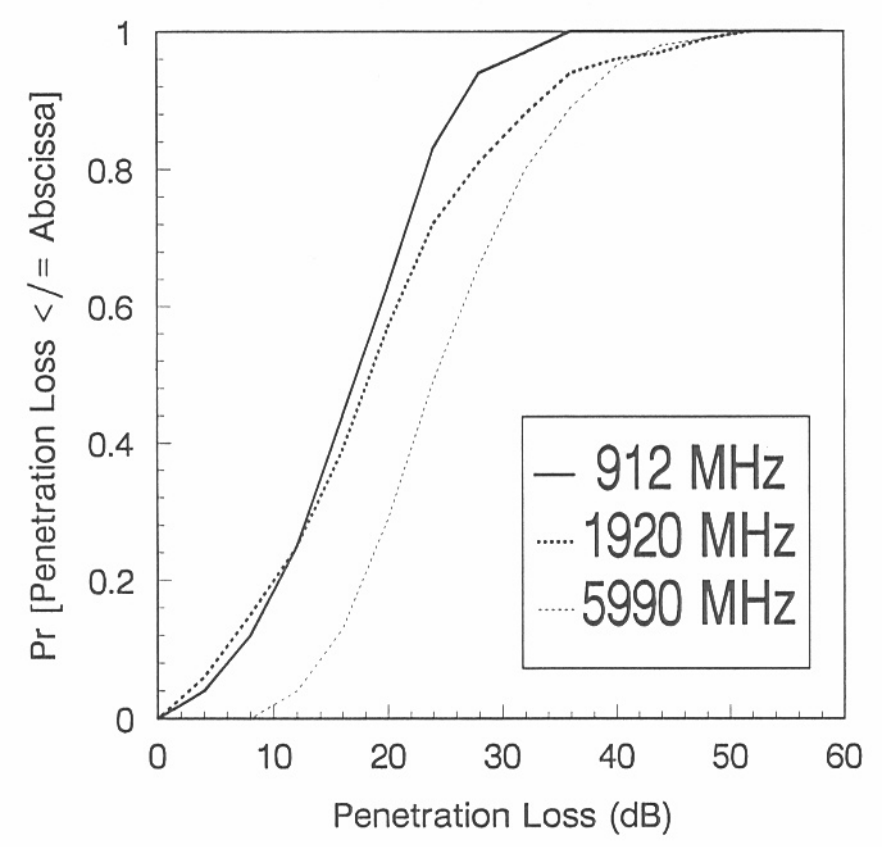

Figure 22. Cumulative probability density functions for NLOS high rise penetration loss.

4.2.1 Penetration Loss into Basements

The LOS building measurements showed greater penetration loss into basements than rooms at ground level. The difference is significant, as illustrated in Table 5. In fact, Cox, et al., recommend that "Because of the large average attenuation into the basement of the house, it does not appear reasonable to combine the basement attenuation statistics with the statistics for the rooms above ground level ([10])." It is, however, essential to incorporate a separate allowance for underground areas in the power requirement equation since PCS users may desire to operate their systems in basements and underground carparks.

Received signal strengths were so low in the underground NLOS high-rise measurements that we could not detect the deep fades at all frequencies. Therefore, the median value of the signal strength in these locations would have been optimistic and not valid for use in comparisons. For this reason, the NLOS underground penetration statistics are not included in this report.

Table 5. Differences Between Mean Ground Floor and Mean Basement LOS Penetration Loss

Frequency (MHz)	Residential (dB)	High Rise (dB)
912	8.7	20.8
1920	17.6	28.8
5990	19.9	34.8

4.2.2 Effects of Building Materials

Histograms of the mean NLOS residential building penetration losses and standard deviations are shown in Figures 23 and 24, respectively.[3] In Figure 24, the standard deviations are high. This is due to the fact that basement measurements have been included in the residential average. Basement penetration loss is significantly higher than the loss in all other rooms (see Table 5) and so causes the standard deviation to be larger.

Residence 1 was brick with wire mesh and plaster. Residence 2 was a tri-level with brick on the first floor and wood on the second. Residence 3 was all brick. Residence 4 was an all brick tri-level. Residence 5 was a two-story house with brick on the first floor, wood on the second floor, a full basement, and the entire house was wrapped with a metallic vapor barrier known as Thermoply®. Residence 6 was a two-story house with brick on the first floor, aluminum siding on the second, and a full basement. Residence 7 was a two-story house with brick on the first floor, wood on the second floor, and a full basement.

Based on the differences in residential building penetration between the three frequencies shown in Figure 23, building walls are frequency selective. This is reasonable because a building wall consists of a dielectric substance containing conducting objects. Such a structure may exhibit frequency-selective behavior, as has been documented by other researchers [1,11]. We also see that lower frequencies penetrate better than higher frequencies. Residence 3 has the highest penetration loss by 5 dB at 5990 MHz; the highest penetration loss by 0.5 dB at 1920 MHz; and the second to lowest penetration loss at 912 MHz. Residence 5 had the highest penetration loss by 3.2 dB at 912 MHz; and the 1920 and 5990 MHz penetration loss for this residence was less than 1.5 dB greater. Residence 2 had relatively low loss at 912 and 1920 MHz; yet "average" loss at 5990 MHz.

[3] Figures 23 and 24 include basement measurements.

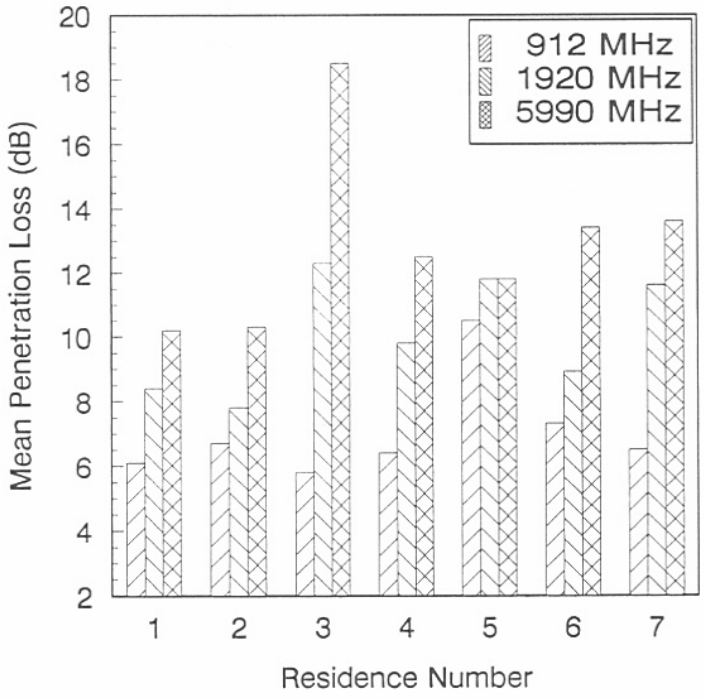

Figure 23. Mean NLOS residential penetration losses.

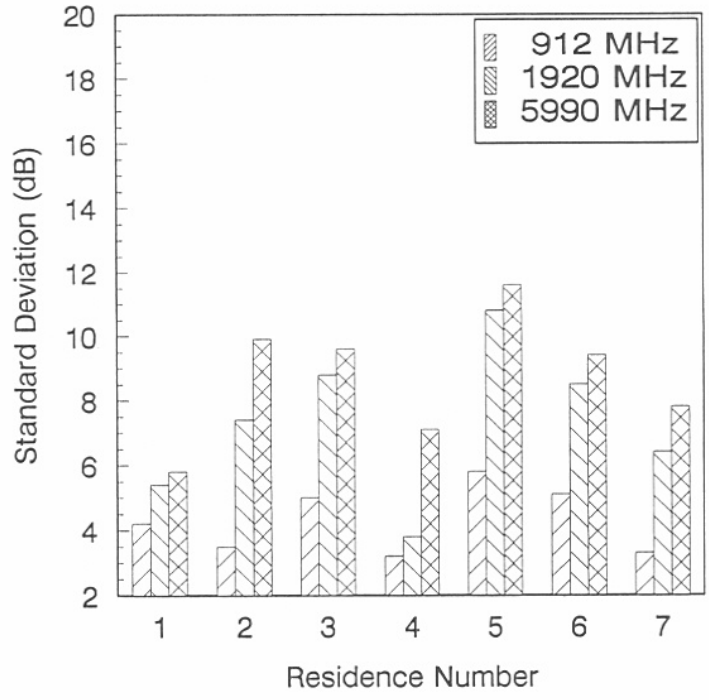

Figure 24. Standard deviations for NLOS residential penetration losses.

4.2.3 Effects of Multistory Buildings

Mean high-rise building penetration loss per floor is shown in Figures 25 through 28. High rises 1 and 4 have lower, more linear penetration losses than high rises 2 and 3. High rises 1 and 4 differ from high rises 2 and 3 in that they span entire city blocks, are newer construction, and contain large walls of glass. Walker reports that windows decrease penetration loss by 6 dB [12]. High rises 2 and 3 are of much older construction, are more closely surrounded by other buildings, have fewer windows, and have much more erratic penetration loss curves. High rise 2 has more windows and lower penetration loss than high rise 3. Figures 29 through 31 show penetration loss at 912, 1920 and 5990 MHz, respectively, for all high-rise buildings measured. The mean values for all data on each floor are indicated by "X's." The "least squares" straight line fit to these means, as calculated by GRAFTOOL™, is also shown on each plot. The slope and first-floor intercept of these lines are given in Table 6.

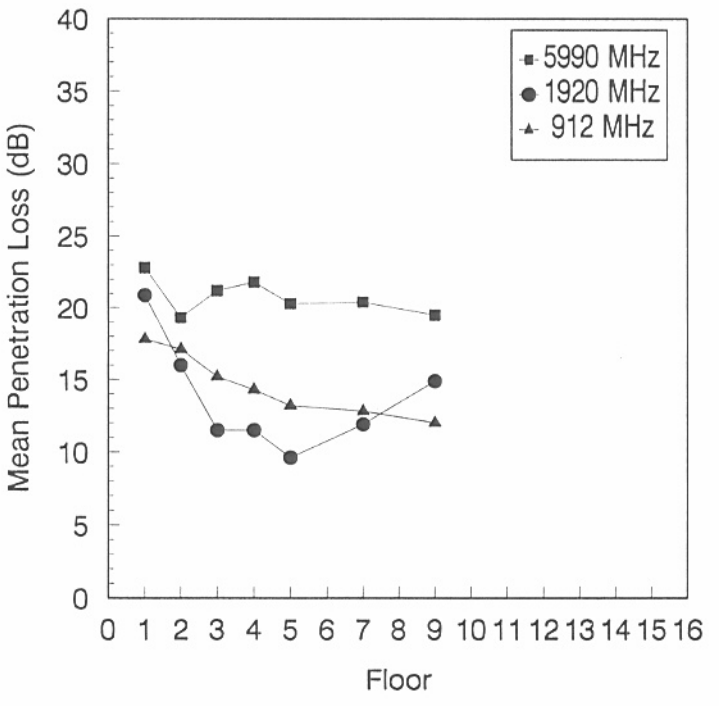

Figure 25. Mean NLOS building penetration losses for high rise 1.

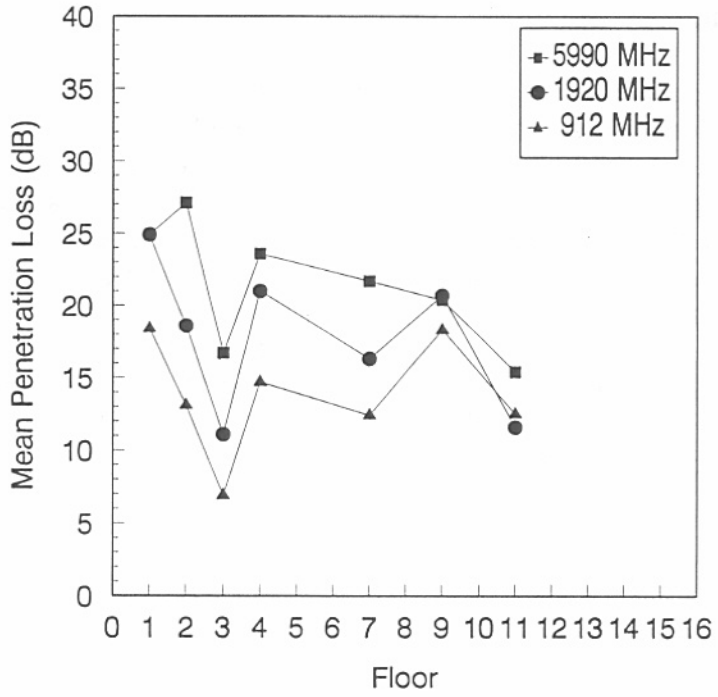

Figure 26. Mean NLOS building penetration losses for high rise 2.

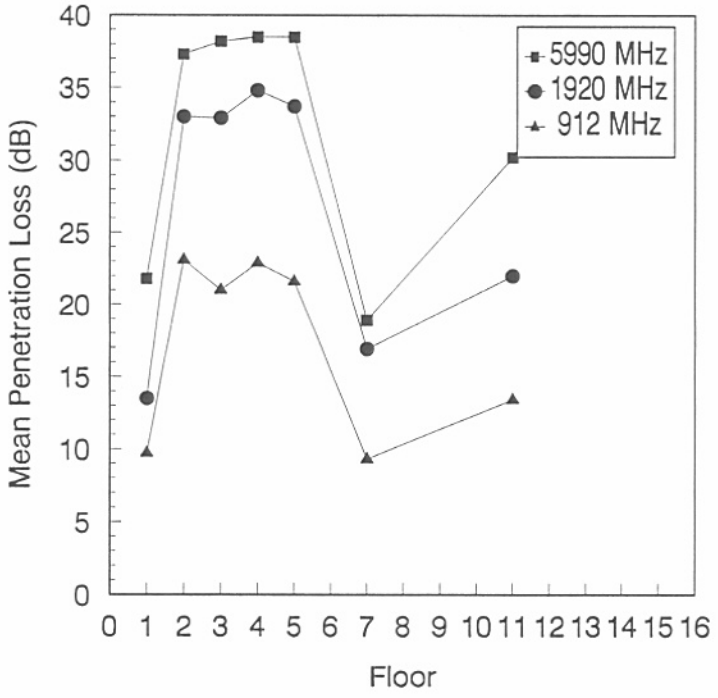

Figure 27. Mean NLOS building penetration losses for high rise 3.

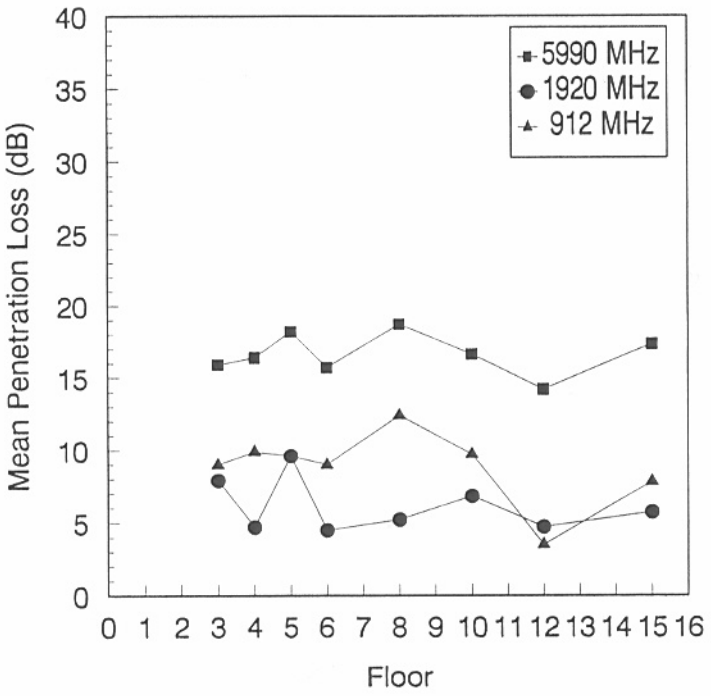

Figure 28. Mean NLOS building penetration losses for high rise 4.

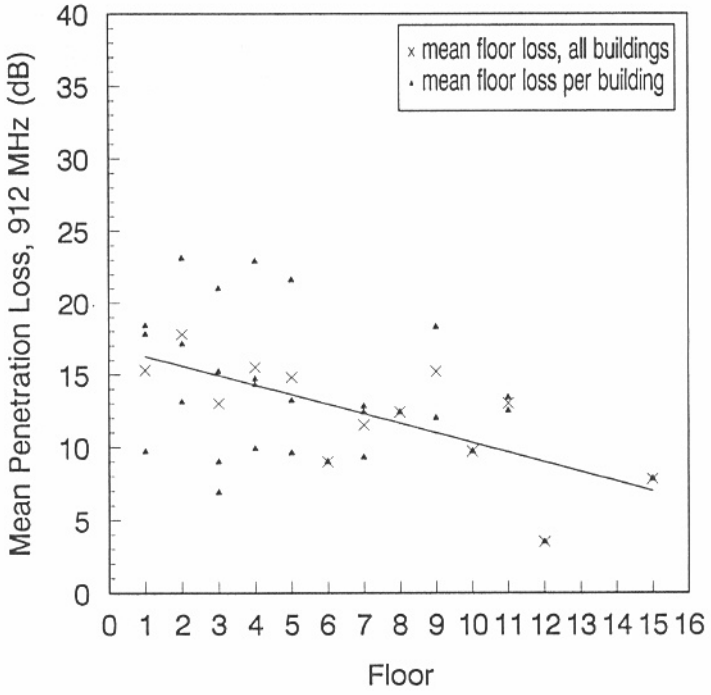

Figure 29. Mean NLOS high rise penetration loss at 912 MHz.

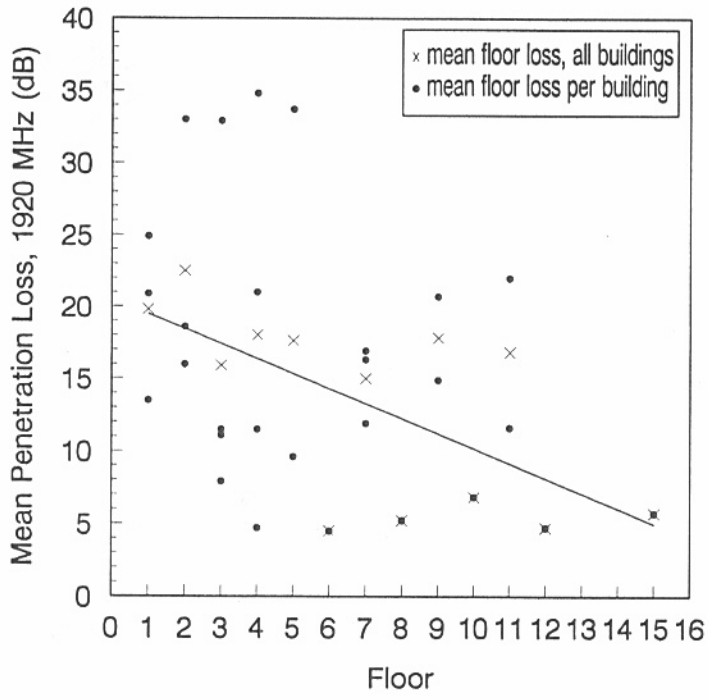

Figure 30. Mean NLOS high rise penetration loss at 1920 MHz.

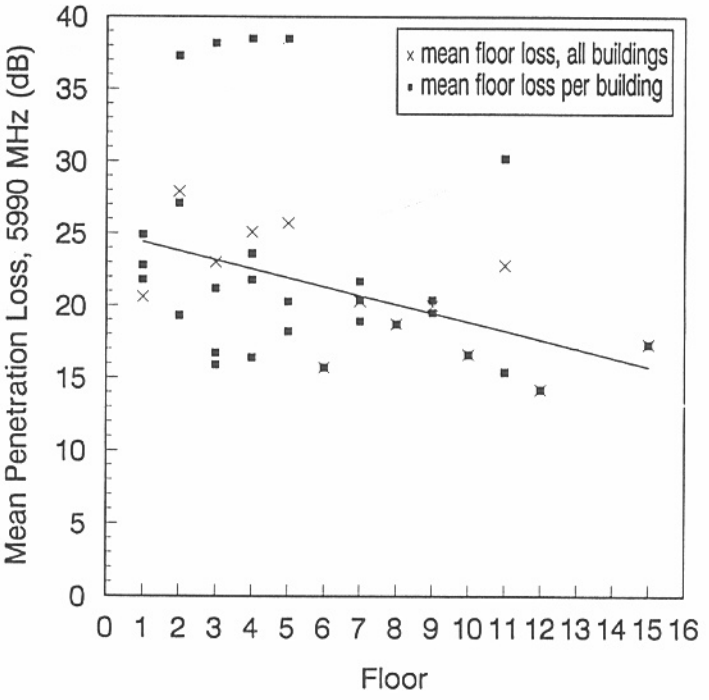

Figure 31. Mean NLOS high rise penetration loss at 5990 MHz.

Table 6. Slope and First Floor Intercept of "Least Squares" Line Fit to Mean Floor Penetration

	912 MHz	1920 MHz	5990 MHz
Slope	-0.66 dB/floor	-1.04 dB/floor	-0.62 dB/floor
Intercept	16.4 dB	19.6 dB	24.5 dB

4.2.4 Effects of Building Shadowing

Shadow loss is the attenuation of a signal due to diffraction around buildings. To calculate building shadowing, outdoor data were collected behind the buildings and subtracted from that collected in front of the buildings (LOS only). Average shadowing loss for each building is given in Table 7. If the building under test were the only building in the vicinity, we would expect the shadowing loss to increase with increasing building height and width, and with increasing frequency. The mean high-rise building shadowing loss is greater than the residential mean and the mean shadowing losses increase with increasing frequency. However, not all highrise buildings have greater shadowing loss than all residences at the same frequency, and shadowing loss does not always increase with frequency even for the same building.

Table 7. Building Shadowing Losses

Site	912 MHz (dB)	1920 MHz (dB)	5990 MHz (dB)
Residence 1	7	4	1
Residence 2	9	10	8
Residence 3	9	19	26
Residence 6	15	19	21
Residence 7	15	17	23
High Rise 1	23	28	25
High Rise 2	35	41	46
High Rise 3	15	14	15
Residential Mean	11	14	16
High-Rise Mean	24	28	29
Building Mean	16	19	21

4.3 Slow Fading Analysis

The variation of the median signal strength about the path loss slope shown in Figure 17 is known as slow fading (also referred to as long-term fading or large-scale variations). Slow fading is typically caused by relatively small-scale variations in topography along the propagation path (i.e., construction materials used in the walls of buildings under test, and shadowing caused by buildings, trees or geographical variations). Knowledge of slow fading characteristics is critical in determining parameters such as required handoff speed and number of handoff requests. Slow fading effects are of particular concern because they generally cannot be eliminated using signal processing techniques such as equalization and coding.

Table 8 shows the standard deviation of the LOS data about the path loss slope. For the residences, standard deviation tends to increase with increasing frequency, whereas for the high rises, there is no increase between 1920 and 5990 MHz. The high-rise buildings show greater standard deviations than the residential buildings at 912 MHz, but this is not true for all buildings at 1920 and 5990 MHz. Some of the residences show higher standard deviations than high rise 1 at 1920, and most of the residences show higher standard deviation than high rise 1 at 5990 MHz. Referring to the environment around the buildings, high rise 1 is located in a relatively open area, with no vegetation in the propagation path. This indicates that any

Table 8. Standard Deviation of LOS Data about the Path Loss Slope

	Standard Deviation (dB)		
	912. MHz	1920 MHz	5990 MHz
Residence 1	6.3	7.4	7.7
Residence 2	6.6	7.5	7.1
Residence 3	7.1	8.9	10.3
Residence 4	6.6	7.9	9.1
Residence 5	7.4	9.8	10.4
Residence 6	7.2	10.2	10.8
Residence 7	7.6	8.7	9.9
High Rise 1	8.8	9.6	9.4
High Rise 2	9.4	11.1	11.0
High Rise 3	12.5	14.5	14.5
High Rise 4	12.1	14.3	13.0

obstruction between the transmitter and receiver is a factor in slow fading. High-rise building shadowing may be a significant factor in long-term fading at these frequencies, but is extremely area-dependent.

4.4 Fast Fading Analysis

The distribution of the fading about the local median is known as fast fading (also referred to as short-term fading or small-scale variations). It is caused by multipath reflections from surrounding objects. This type of fading is extremely rapid, with the possibility of very deep fades every half-wavelength. Figure 32 shows an example of our raw data. This figure shows fading measured with respect to time. The time elapsed for this sample was 10 s and the distance travelled was approximately 8 m. As seen here, fast fades occur more often, but for a shorter duration, at the higher frequency. Knowledge of fast fading characteristics is critical in determining adequate signal-to-noise ratios, and in designing optimum error-correction algorithms.

To calculate the fast fading distributions from the measured data, we subtracted each raw measured value from the mean of the room or corner. This removed the slow-fading component from the data, leaving only the fast-fading component for processing.

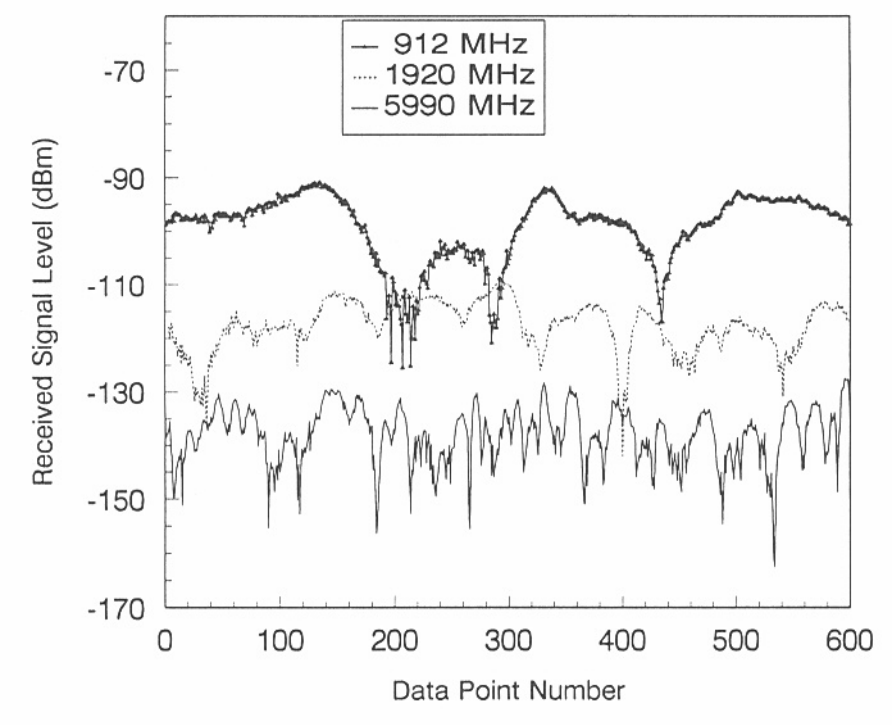

Figure 32. Example of raw data showing fast fading.

Figures 33 and 34 show fast fading cumulative probability distribution functions for residence 7, LOS, and high rise 3, NLOS, respectively. For both buildings, all three frequencies tend towards the same distribution shape. Fast fading is generally accepted to be Rayleigh distributed at distances of greater than 2 km, becoming less so and tending toward Rician distribution at closer proximities [13].

4.5 Correlation Analysis

Making simultaneous measurements at three frequencies allows a meaningful comparison of the three received signals. If a large correlation (i.e., close to 1.0) exists between any of these frequencies, then future measurements need only be collected at one frequency, and results could be extrapolated to another frequency or frequencies.

Figures 35, 36, and 37 compare the mean residential NLOS penetration losses between 912 and 1920 MHz, between 1920 and 5990 MHz, and between 912 and 5990 MHz, respectively. The graphs use one point per room and combine the results of seven houses. Figures 38, 39, and 40 compare the same parameters for the high-rise buildings, using one point per floor to combine the results of all four NLOS high-rise measurements. The regression line shown on the above graphs is the regression line as calculated by GRAFTOOL™ such that the deviation of the raw data points from the function is minimized. The correlation coefficients of the mean NLOS residential and high-rise building penetration losses are shown in Table 9.

Table 9. Correlation Coefficients of Linear Regression Between Frequencies

Frequencies (MHz)	Residential	High Rise
912 and 1920	.919	.928
912 and 5990	.763	.783
1920 and 5990	.942	.932

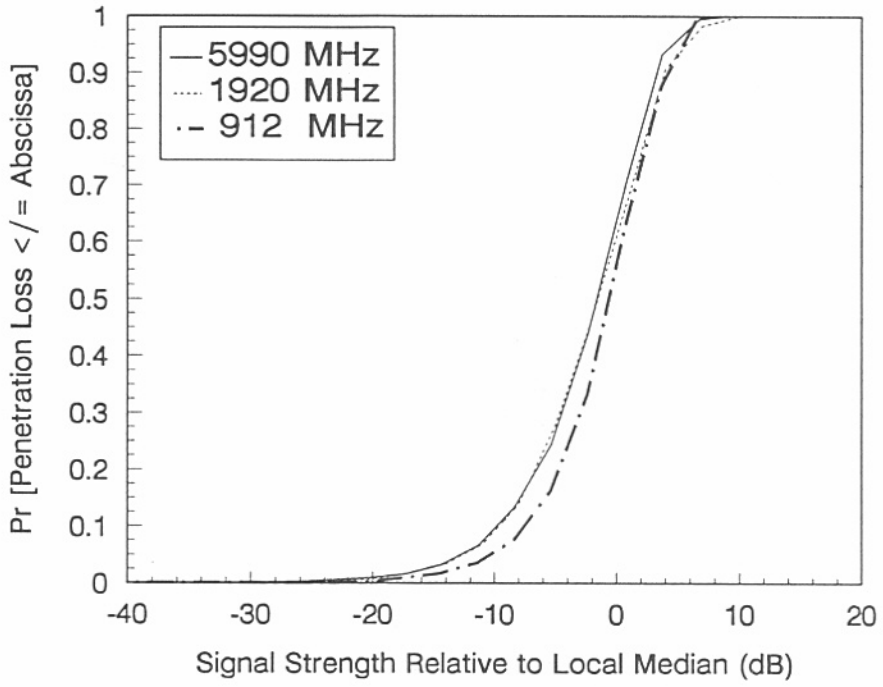

Figure 33. Cumulative probability functions for residential fast fading

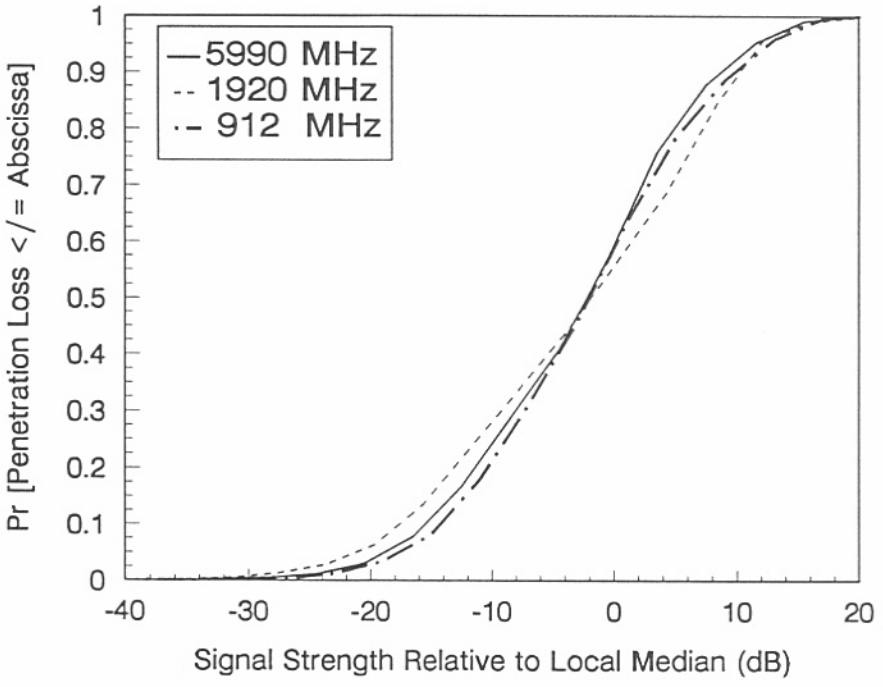

Figure 34. Cumulative probability distributions for high rise fast fading

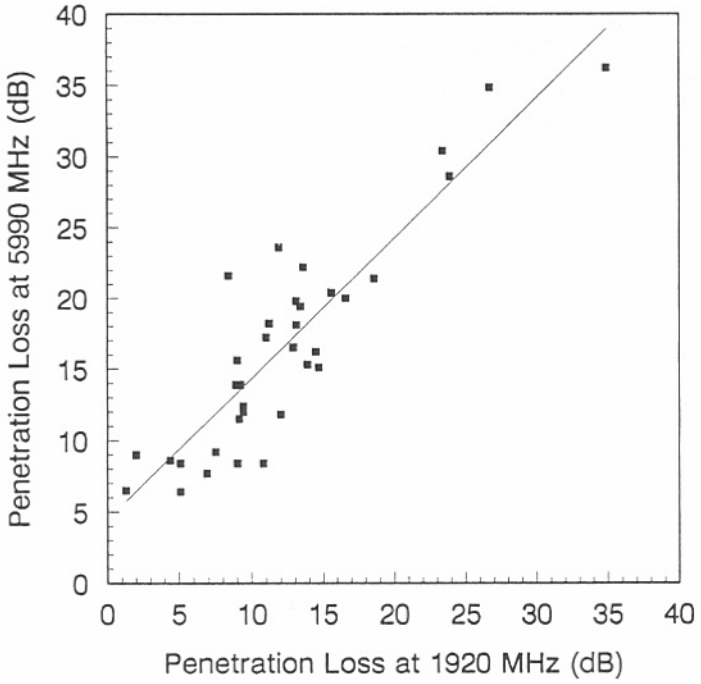

Figure 35. Comparison between 912 and 1920 MHz mean NLOS residential penetration losses.

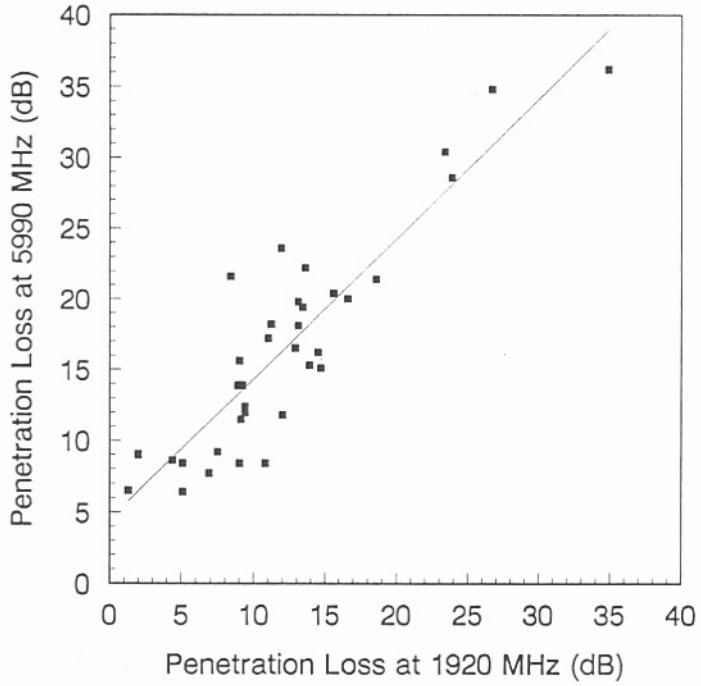

Figure 36. Comparison between 1920 and 5990 MHz mean NLOS residential penetration losses.

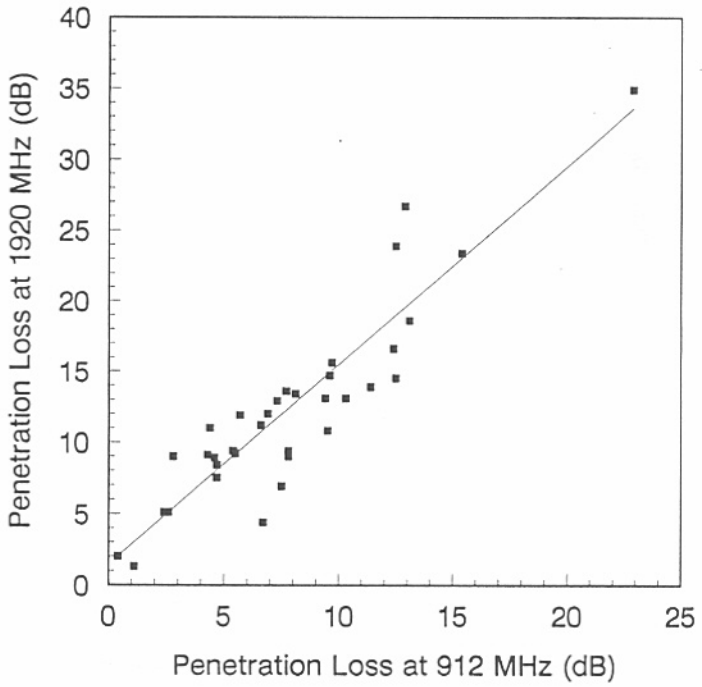

Figure 37. Comparison between 912 and 5990 MHz mean NLOS residential penetration losses.

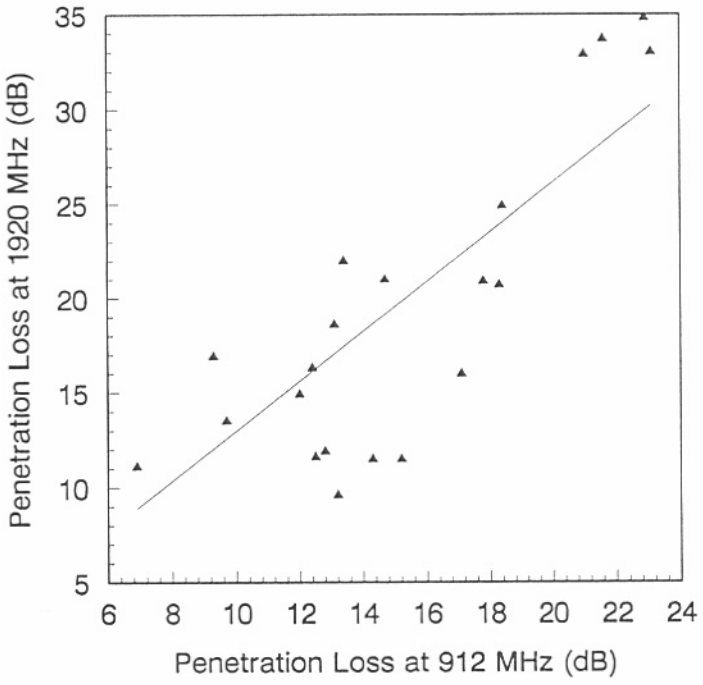

Figure 38. Comparison between 912 and 1920 MHz mean NLOS high rise penetration losses.

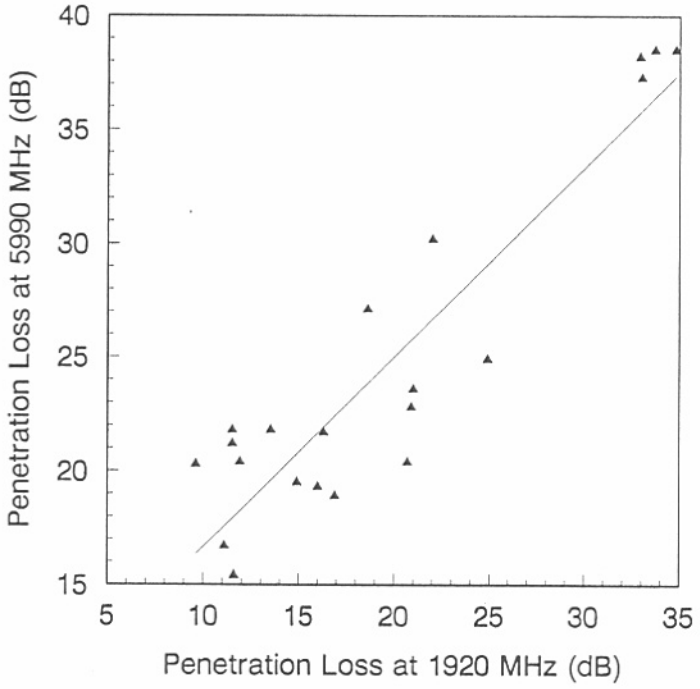

Figure 39. Comparison between 1920 and 5990 MHz mean NLOS high rise penetration losses.

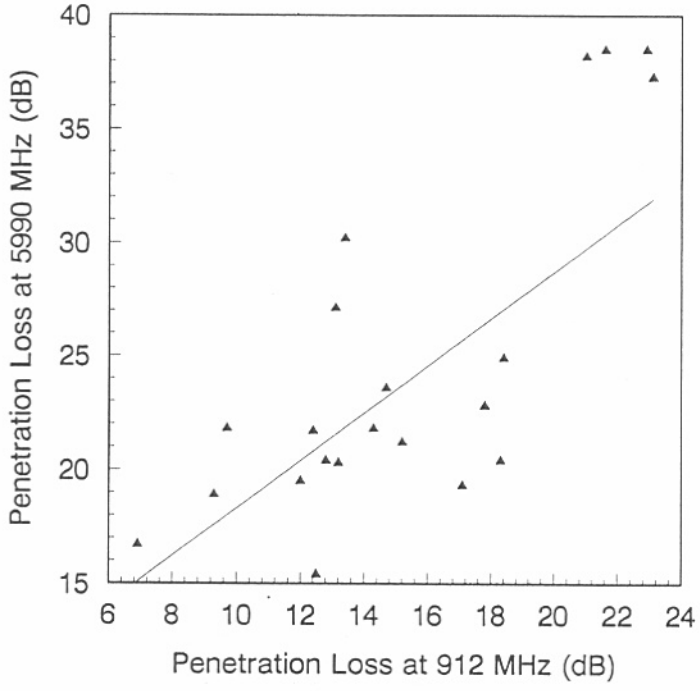

Figure 40. Comparison between 912 and 5990 MHz mean NLOS high rise penetration losses.

5. SUMMARY AND CONCLUSIONS

This report describes building penetration measurements conducted simultaneously at 912, 1920, and 5990 MHz. Eleven environments were measured, representing typical residential and high-rise buildings. Measurements were taken on all levels of the residential buildings, and seven or eight nonsequential levels of the high-rise buildings, up to a maximum of the fifteenth level. The measurement system consisted of a narrowband, fixed, outdoor transmitter and a mobile indoor receiver. The transmit and receive antennas were identical biconical, vertically polarized, omnidirectional antennas. From the data collected, we analyzed path loss distributions, penetration losses, building shadowing loss, loss into basements, slow fading, fast fading, and variations in loss due to frequency, building height, and building construction materials. A relationship between the data from the three frequencies was shown by way of correlation coefficients.

Path loss distributions

Although other researchers have described path loss into buildings as following a log-normal distribution [14, 15, 16], our data (see Appendix C) show no clear, consistent distribution. Although some of the distributions tend toward Gaussian or Rayleigh, many are bi-modal. The bi-modal distributions in the residences are caused by the fact that the basement path loss was significantly higher than the loss measured in the rest of the building. The bi-modal distributions seen in the high rise 2 and 3 LOS measurements are caused by the fact that only two corners of the building could be LOS to the transmitter, and therefore measurements were made in only these two corners.

Penetration loss

Penetration losses were calculated for each building from the path loss data collected. Penetration loss was found to vary with building location, construction material, frequency, and building level measured. The average penetration losses for all buildings was 8.2, 9.8, and 14.1 dB at 912, 1920, and 5990 MHz, respectively.

Penetration into basements

Signal penetration into basements was measured to be 8.7, 17.6, and 19.9 dB lower than penetration into the ground floor of the residences at 912, 1920, and 5990 MHz, respectively. LOS penetration into high-rise building basements was 20.8, 28.8, and 34.8 dB less than penetration at 912, 1920, and 5990 MHz, respectively. It is essential to incorporate a separate allowance for basements in the power requirement budget or to position additional transmitters in these areas if there is a desire to use PCS systems in basements and underground carparks.

Building construction variations

The high-rise building measurements consistently showed greater building penetration loss than the residential buildings. Presumably this is due to the use of steel frames and thicker walls of masonry or concrete in the high-rise buildings. We found the difference in median penetration loss at 912, 1920, and 5990 MHz to be 4.8, 3.5, and 8.3 dB greater, respectively, in the high-rise environment than in the residential environment.

Base antenna height considerations

The low base antenna height used for these measurements affected the path loss distribution and the frequency dependency of the penetration loss. When the base antenna height is low, penetration is mainly via walls and windows, and therefore the construction material of the building becomes more significant. This can create more variation in penetration loss at different frequencies, as the building materials can be frequency selective. The low base antenna height also leads to an increase in building shadowing, depending on the surrounding environs. This can create more variation in received signal level, but only affects penetration losses when the reference signal (ground level) experiences shadowing effects and the upper floors of the building under test do not. With a low base antenna height, the upper floors experienced similar shadowing effects, and so our measured penetration loss slopes (Figures 29-31) were less steep (see summary of building height dependency), and did not change after the fifth floor as found by other researchers. The low base antenna height does lead to increased shadowing effects and hence reduced signal levels inside the building, which will require either more base stations per city or increased transmitter power at each one.

Frequency dependency

The frequency variation of penetration loss appears to be largely dependent on building construction. For residential buildings, mean penetration losses increased as frequency increased, as found in [17]. However, not all the high-rise buildings followed this pattern. For most floors of high-rise buildings 1 and 4 (which had primarily glass walls), the 1920-MHz signal encountered less penetration loss than the 912-MHz signal. Tanis [18], and Davidson and Marturano [19] measured commercial building penetration losses that decreased as the frequency increased. Davidson and Marturano explained this apparent contradiction as a difference in building materials. Penetration into residences is primarily through the windows, walls and roof. Loss through these materials is relatively low and increases with increasing frequency. Both Tanis and Davidson and Marturano measured industrial buildings of reinforced concrete where the dominant penetration was through slots (windows and cracks). Loss through these materials decreases with increasing frequency. Allen, et al. [20] also found decreasing loss with increasing frequency for penetration through a metal building. Here, also, the dominant penetration is through slots (small windows, ducts and holes).

Building height dependency

For the high-rise buildings, NLOS penetration loss decreased 0.6 to 1 dB per floor as building floor level increased. Note that for all floors measured, the reference was always at street level. Most researchers [21, 22, 23, 24, 25, 26, 27, 28, 29] have observed that building penetration losses decrease 1 to 3 dB per floor for the first five or six floors of high-rise buildings. This difference in slope is probably due to the low transmitter height we used, causing the obstructions between transmitter and receiver to be more consistent, and the slope less steep. Transmitters placed on rooftops may have fewer obstructions to the upper floors of buildings than to the lower floors. Decreases in penetration loss are seen on the upper floors of high-rise buildings in urban environments [23], as opposed to high-rise buildings in suburban environments [12]. The penetration characteristics of buildings in urban areas depend highly on the surrounding structures, and are much harder to predict than for high-rise buildings in

suburban environments. A couple of authors even noted penetration loss that increases at higher floor levels [11,12]. It is interesting to note that no matter what the pattern of the penetration loss versus floor level, all frequencies exhibit the same overall variation (Figures 25-28).

Building shadowing

The mean high-rise building shadowing loss is greater than the residential mean and the mean shadowing losses increase with increasing frequency. However, not all high-rise buildings have greater shadowing loss than all residences at the same frequency, and shadowing loss does not always increase with frequency even for the same building. This is due to the effects of multipath from the surrounding reflectors, such as buildings, geographical structures, vehicles, and vegetation; as well as the construction materials and contents of the building. Building shadowing loss is as dependent on the features of the area surrounding the building as it is on the building itself.

Slow fading analysis

Slow fading analysis reveals that any obstruction in the propagation path is a factor in long-term fading. Slow fading is frequency dependent and increases with increasing frequency in the residential building environment. In the high-rise environment, long-term fading is more difficult to analyze. Building shadowing loss may be a significant factor at these frequencies, but is extremely area-dependent.

Fast fading analysis

The fast fading characteristics of building penetration shows a tendency for all frequencies to have the same distribution shape, especially in the residential building. Deep fades occur more frequently as the frequency increases, but for a shorter duration.

Regression analysis

We observed strong linear correlations, greater than 0.90, between the penetration losses at 912 and 1920 MHz, and between 1920 and 5990 MHz. This opens the possibility of measuring building penetration loss at one frequency and extrapolating to find the penetration loss at other frequencies. The correlation between 912 and 5990 MHz, however, was less than 0.80, and so extrapolation between these two frequencies is not expected to be as accurate.

Implications of measurements

The ability to use the same mobile communications system in an uninterrupted manner both inside and outside buildings would be advantageous to PCS subscribers. If outdoor base stations can provide coverage to indoor users, handoff and its related difficulties are eliminated. Locating base stations on existing structures such as street or traffic lights has obvious economic advantages. The penetration loss measurements presented can be used to determine the feasibility of outdoor-to-indoor personal communication links. The cumulative distribution functions can provide link margin information to PCS designers. If building penetration losses of the magnitude presented in this paper can be tolerated by a PCS system, then there exists the possibility of using low-height base stations for transmission to indoor subscribers.

6. ACKNOWLEDGMENTS

The sponsorship, support, and useful insight in the reduction of the data provided by Sergio Aguirre of US WEST Technologies, Inc., and the technical assistance provided by Ken Allen (NTIA/ITS) are greatly appreciated. We extend much appreciation to Jim Washburn, Mike Cotton, Eric Loew, Hans Liebe, Frank Sanders, Ken Allen, Tom Brawley, and Richmond Homes, Inc. for permitting the residential measurements reported in this paper to be made in their homes. We also thank Judy Richardson, Fred Gurule, and Ron Minks for graciously allowing us access to the high-rise buildings, and Ed Potter, Eric Potter, and Louie Ruiz for reserving specific parking spaces for us in their parking lots. The measurements were funded by US WEST Technologies, Inc., under a Cooperative Research and Development Agreement.

7. REFERENCES

[1] CCIR, "Propagation data and prediction methods for the terrestrial land mobile service using the frequency range 30 MHz to 3 GHz," Report #567-4, Reports of the CCIR, Annex to Volume V, Propagation on Non-Ionized Media, pp. 335-336, 1990.

[2] W.J. Tanis II, "Bell Atlantic Mobile Systems PCS Propagation Research," Fifth Quarterly Report to the Federal Communications Commission (FCC), p. 13, Feb. 1993.

[3] W.J. Tanis II, "Bell Atlantic Mobile Systems PCS Propagation Research," Fifth Quarterly Report to the FCC, p. 23, Feb. 1993.

[4] V. Erceg, S. Ghassemzadeh, M. Taylor, D. Li, and D. L. Schilling, "Urban/suburban out-of-sight propagation modeling," *IEEE Comm. Mag.*, pp. 56-61, June 1992.

[5] J.D. Parsons, *The Mobile Radio Propagation Channel,* New York: John Wiley & Sons, 1992, pp. 24-26.

[6] W.J. Tanis II, "Bell Atlantic Mobile Systems PCS Propagation Research," Fifth Quarterly Report to the FCC, p. 26, Feb. 1993.

[7] P.E. Mogenson, P. Eggers, C. Jensen, and J.B. Anderson, "Urban area radio propagation measurements at 955 and 1845 MHz for small and micro cells," in *IEEE Global Telecomm. Conf. Digest,* Phoenix, AZ, Dec. 1991, pp. 1297-1302.

[8] E. Moriyama, T. Iwama, and T. Saruwatari, "Experimental investigation of 1.5 GHz and 2.6 GHz band land mobile radio propagation in urban and rural area," in *Proc. 39th Veh. Tech. Conf.,* Apr. 1989, pp. 311-315.

[9] K. Low, "Comparison of urban propagation models with CW-measurements," in *IEEE Veh. Tech. Conf. Digest,* May 1992, pp. 936-942.

[10] D.C. Cox, R.R. Murray, and A.W. Norris, "Measurements of 800-MHz radio transmission into buildings with metallic walls," *Bell Sys. Tech J.,* vol. 62, No.9, pp. 2695-2717, Nov. 1983.

[11] A.F. deToledo and A.M.D. Turkmani, "Propagation into and within buildings at 900, 1800 and 2300 MHz," in *IEEE Veh. Tech. Conf. Digest,* May 1992, pp. 633-636.

[12] E.H. Walker, "Penetration of radio signals into buildings in the cellular radio environment, *"Bell Sys. Tech. J.*, Vol. 62, No.9, pp. 2719-2734, Nov. 1983.

[13] W.J. Tanis II, "Bell Atlantic Mobile Systems PCS Propagation Research," Fifth Quarterly Report to the FCC, pp. 29-31, Feb. 1993.

[14] R. Bownds, "Measurements of propagation from street microcells into buildings at 900 and 1700 MHz," Ericsson Report S/DT 92:138, Sweden, Aug. 1992.

[15] L.P. Rice, "Radio Transmission into Buildings at 35 and 150 MHz," *Bell Sys. Tech. J.*, Vol. 38, p. 199, Jan. 1959.

[16] D.C. Cox, R. Murray, and A.W. Norris, "800 MHz attenuation measured in and around suburban houses," *AT&T Bell Labs Tech. J.*, Vol. 63, No. 6, pp. 921-954, July/Aug. 1984.

[17] P.I. Wells, "The Attenuation of UHF Radio Signals by Houses," *IEEE Trans. on Veh~ Tech.*, Vol. VT-26, No.4, pp. 358-362, Nov. 1977.

[18] W.J. Tanis II, "Bell Atlantic Mobile Systems PCS Propagation Research," Fifth Quarterly Report to the FCC, p. 7, Feb. 1993.

[19] A. Davidson and L. Marturano, "Impact of Digital Techniques on Future LM Spectrum Requirements," *IEEE Veh. Tech. News*, Vol. 40, No.2, pp. 14-30, May 1993.

[20] K.C. Allen, N. DeMinco, J.R. Hoffman, Y. Lo, and P.B. Papazian, "Building penetration loss measurements at 900 MHz, 1.4 GHz, and 28.8 GHz," NTIA Report 94-306, May 1994 (NTIS Order No. PB 94204781).

[21] D.C. Cox, R. Murray, and A.W. Norris, "Antenna height dependence of 800 MHz attenuation measured in houses," *IEEE Trans. on Veh. Tech.*, VT-34, pp. 108-115, May 1985.

[22] R.C.V. Macario, "How Building Penetration Loss Varies with Frequency," *IEEE Veh. Tech. News*, Vol. 40, No. 6, pp. 26-27, Nov. 1993.

[23] W.J. Tanis II, "Bell Atlantic Mobile Systems PCS Propagation Research," Fifth Quarterly Report to the FCC, p. 9-10, Feb. 1993.

[24] W.C.Y. Lee, *Mobile Cellular Telecommunications Systems*, New York: McGraw-Hill Book Co., 1989, pp. 104-105.

[25] P.J. Barry and A.G. Williamson, "Statistical model for UHF radio-wave signals within externally illuminated multistory buildings," *IEE Proceedings*, vol. 138, No. 4, Aug. 1991.

[26] B. Benzair, V.S.M. Renduchintala, H. Smith, and D.H. Williams, "Satellite paging experiments into buildings," in *Proc. of IEE Colloquium on University Research into Mobile Radio*, London, UK, 1990.

[27] S. Mockford and A. Turkmani, "Penetration loss into buildings at 900 MHz," in *Proc. of IEE Colloquium on Propagation Factors and Interference Modeling for Mobile Radio Systems*, London, UK, 1988.

[28] A.F. deToledo, D.G. Lewis, and A.M.D. Turkmani, "Radio propagation into buildings at 1.8 GHz," in *Proc. of IEE Colloquium on University Research in Mobile Radio*, London, UK, 1990.

[29] A.M.D. Turkmani and A.F. deToledo, "Radio transmission at 1800 MHz into, and within, multistory buildings," *IEE Proceedings*, vol. 138, No. 6, Dec. 1991.

8. BIBLIOGRAPHY

[1] European Cooperation in the Field of Scientific and Technical Research, Technical Document 231, "Building penetration losses," "Propagation models" Subgroup, COST 231 TD (90) 116 Rev. 1, Florence, Jan. 1991.

[2] S. T. Chia, "1700 MHz urban microcells and their coverage into buildings," in *Proc. of IEE 7th International Conference on Antennas and Propagation,* ICAP 91, London, UK, Apr. 1991.

[3] R.V. Hogg and E.A. Tanis, *Probability and Statistical Inference,* New York: Macmillan Publishing Co., Inc., 1977.

[4] D. Molkdar, "Review on radio propagation into and within buildings," *IEE Proceedings-H,* Vol. 138, No. 1, Feb. 1991.